1051

Commission of the European Community

JOINT
RESEARCH
CENTRE

NEANDC (E) 212 "U" Vol. III Euratom
INDC (EUR) 013/G

ANNUAL PROGRESS REPORT ON NUCLEAR DATA

1979

NDS LIBRARY COPY

CENTRAL BUREAU FOR NUCLEAR MEASUREMENTS

GEEL (BELGIUM)

June 1980

TABLE OF CONTENT

1. NUCLEAR DATA

1.1 NEUTRON DATA

1.1.1 *Actinides*

Fission and absorption cross sections of ^{241}Am

G. Van Praet, E. Cornelis, F. Poortmans, S. Raman, G. Rohr, J.A. Wartena, H. Weigmann

(WRENDA 76/77: 1038, 1042, 1046)

A first series of measurements on a 1.7 g metallic ^{241}Am sample obtained from ORNL, were made. These include measurements of the absorption cross section from ~ 5 eV to 100 keV and of the fission cross section in the resonance region (5 eV to ~ 100 eV). Analysis of the fission data showed that the liquid scintillator detector has some residual γ-efficiency (~ 1 % of its efficiency for fission neutrons) probably due to a disturbance of the pulse shape discrimination circuits by the high background level. Analysis of the absorption cross-section data has been started. The continuation of the measurement programme will be decided after first results from the analysis of the absorption data have been obtained.

Measurement of the Neutron Induced Fission Cross Section and of the Spontaneous Fission Half-Life of ^{240}Pu

C. Budtz-Jørgensen, H.-H. Knitter, M. Mailly, R. Vogt

(WRENDA 76/77: 962 to 971)

a) Measurement at the Van de Graaff

The fission cross section of ^{240}Pu was measured in a back-to-back geometry relative to the fission cross section of ^{235}U in the energy range from 140 keV to 9.75 MeV. The fission events were registered by fragment detection with the help of parallel plate ionization chambers. The fission layers of ^{235}U and ^{240}Pu have a diameter of 2.8 cm and a thickness of 200 $\mu g/cm^2$ and of 50 $\mu g/cm^2$ respectively, and they are positioned at a distance of 6 cm from the neutron producing target and at zero degree with respect to the incident ion beam of the Van de Graaff accelerator. In order to avoid alpha pulse pile-up problems from the ^{240}Pu sample a special chamber described elsewhere in this report was used. The Van de Graaff was operated in pulsed mode and at each incident neutron energy time-of-flight spectra were recorded for the fission of ^{235}U and of ^{240}Pu respectively. A neutron time-of-flight detector was used to check the monoenergetic neutron beam. The time-of-flight spectra allowed one to obtain the count rate ratio corrected for time-uncorrelated background and for the events from spontaneous fission.

At energies below 1.10 MeV measurements were made using the $^{7}Li(p,n)^{7}Be$ neutron producing reaction, employing LiF-targets about 20 keV thick and experimental data were taken in steps of about 20 keV neutron energy.

In the neutron energy range from 1.0 MeV to 4.0 MeV the $T(p,n)^3He$ reaction was used to produce the neutrons. Between 1.0 MeV and 2.0 MeV and between 2.0 MeV and 4.0 MeV measurements were made in 50 keV and 100 keV intervals using T-Ti targets of 0.4 and 2.0 mg/cm^2 respectively. Above 4.0 MeV the $D(d,n)^3He$ reaction was used in conjunction with a deuterium gas target.

The energy spread of the neutrons varied with neutron energy from about 120 keV at 4 MeV to 45 keV at 9.75 MeV. Measurements were made with and without deuterium gas in the cell, in order to correct for fission events which were not induced by neutrons from $D(d,n)^3He$ reaction. In this energy range from 4 MeV to 9.75 MeV experimental data were taken in incident neutron energy steps of 200 keV. The results of these measurements are shown in Fig. 1.1.1.

The overall uncertainty of the data is 3 %. The agreement with data of Behrens et al. and Cierjacks et al. is good.

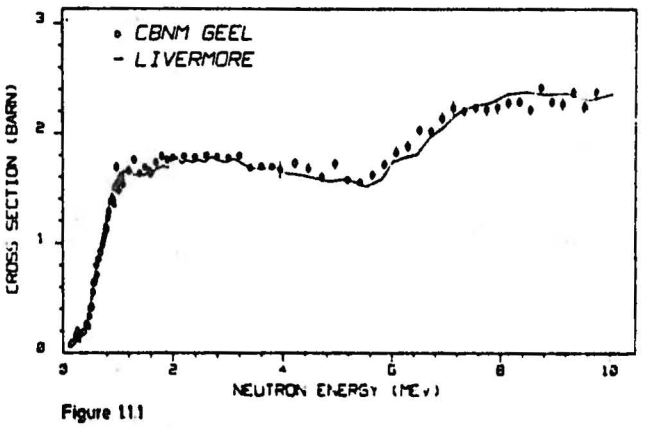

Figure 1.1.1

The results available in the literature for measurements of the spontaneous fission half life lie between 1.20 10^{11} and 1.45 10^{11} years. Many of the results do not agree with each other within the quoted errors. Therefore we evaluated from a fragment spectrum of the spontaneous fission of ^{240}Pu, the spontaneous fission half life. The value $T_{SF} = (1.15 \pm 0.03) \cdot 10^{11}$ years is in disagreement with the value of $(1.31 \pm .05) \times 10^{11}$ years proposed at "The first coordinated Research Meeting of Transactinium Isotope Nuclear Data", IAEA, Vienna, 20-21 April 1978, INDC(NDS)-96/N, p. 10.

b) *Measurements at the Linac*

A fission chamber similar to the one mentioned above was mounted at a 8 m flightpath station at the Linac. Measurements of the neutron induced fission cross section of ^{240}Pu relative to the fission cross section of ^{235}U were performed with the following Linac parameters: 10 ns pulse width, 800 Hz repetition frequency and 3.6 kW mean beam power. The neutron flight times and the energies of the fission fragments were analysed and stored by the multi parameter data acquisition and processing system "Nuclear Data 6660".

The measurements at the Linac are completed and the analysis of the available data has been started. Fig. 1.1.2. shows part of the fission cross section results of ^{240}Pu obtained in the region between 10 keV and 300 keV. One can see a complex structure and strong variations of the subthreshold fission cross section near to the threshold, hitherto not observed in ^{240}Pu.

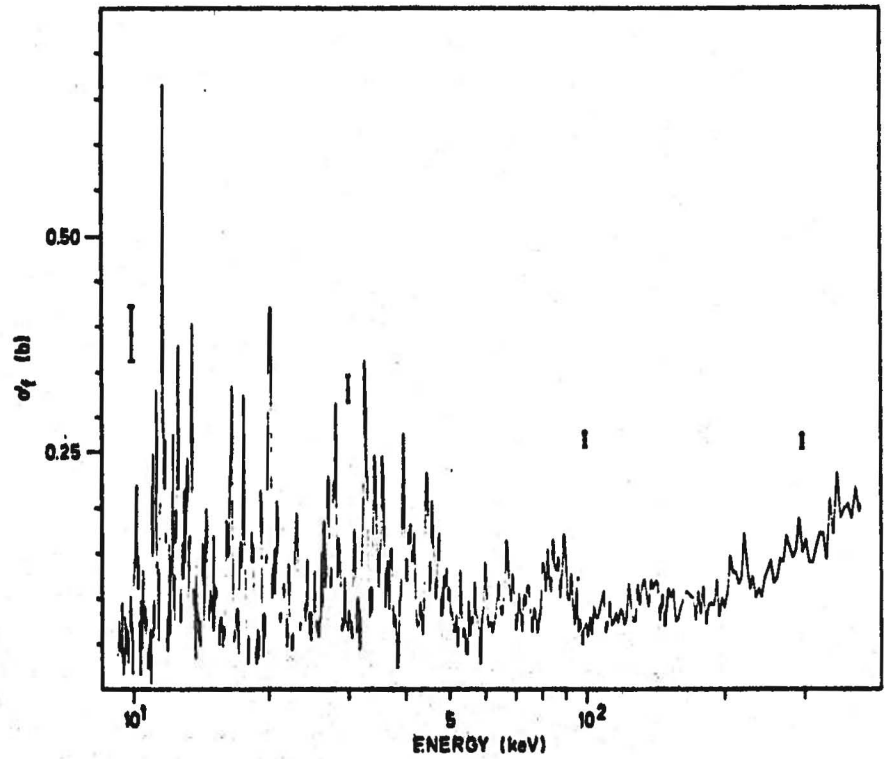

Figure 1.1.2 Fission cross section of ^{240}Pu in the neutron energy range from 10 to 300 keV and the associated representative error bars.

Measurement of the $^{239}Pu(n,f)$ cross section from thermal up to 30 keV neutron energy

C. Wagemans, G. Coddens, M. Barthélémy, J.A. Wartena, H. Weigmann

(WRFNDA 76/77: 911 - 913)

Measurements of the ^{239}Pu fission cross-section were performed covering the neutron energy region from thermal up to 30 keV. Fission fragments as well as fission neutron detection techniques were used. Also for the neutron flux determination different methods were applied. From the σ_f-data, several fission integrals were calculated and compared with other results.

Fission Fragment Mass- and Energy- Distributions for the Neutron Induced Fission of ^{239}Pu as a function of the Resonance Spins

C. Wagemans, G. Wegener-Penning, H. Weigmann, R. Barthélémy

Measurements were performed at an 8 m flight-path of LINAC to study the fission fragment mass- and energy-distributions for $^{239}Pu(n,f)$ as a function of the neutron energy. A ^{239}Pu-layer on a transparent backing was mounted in a vacuum chamber and bombarded with neutrons with energies from 2.10^{-2} eV up to about 10^6 eV. The pulse-height spectra of coincident fission fragments were measured with cooled surface barrier detectors. With the mass- and momentum conservation relations, and using the Schmitt-Neiler calibration method to convert the measured pulse-heights into energy, fission

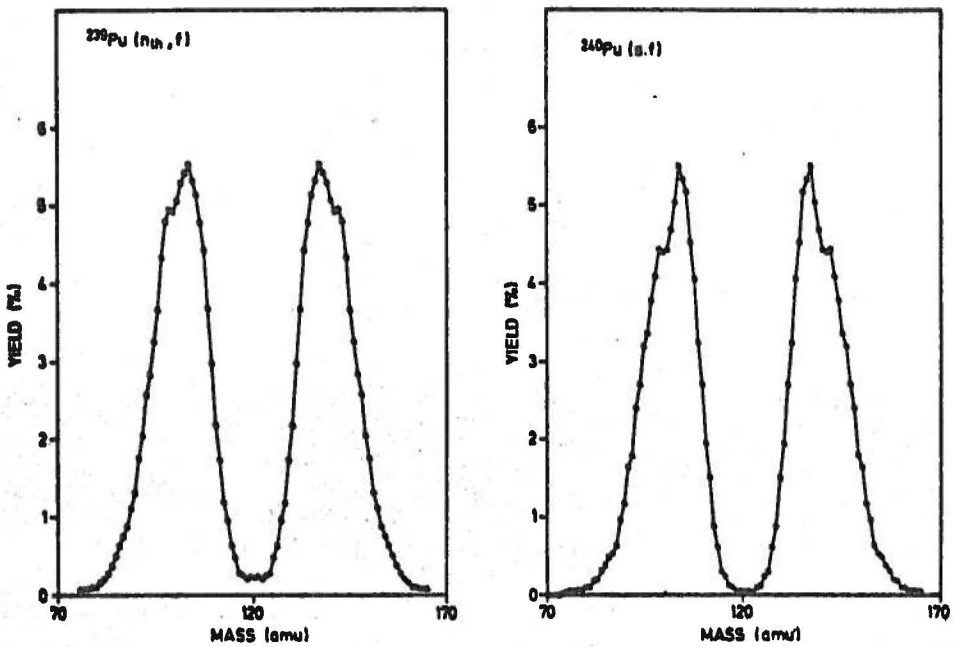

Figure 1.1.3 Fission fragment mass-distributions for the thermal neutron induced fission of ^{239}Pu and for the spontaneous fission of ^{240}Pu.

TABLE 1.1.1.

Mean Total Kinetic Energy and Mass-Values for the $^{239}Pu(n,f)$-Resonances

E_n(eV)	J	$\bar{E}_K^*$ (MeV)	$\bar{m}_L^*$	$\bar{m}_H^*$
7.82	1	178.13 ± 0.07 b)	100.74	139.26
10.93	1	178.00 ± 0.07	100.85	139.15
11.89	1	178.06 ± 0.13	100.94	139.06
14.31 14.68	1	178.06 ± 0.09	100.79	139.21
15.46	0	178.01 ± 0.18	100.73	139.27
17.66	1	178.10 ± 0.13	100.84	139.16
26.24	1	177.93 ± 0.15	100.78	139.22
32.31	0	178.21 ± 0.26	100.88	139.12
41.5 a)	1	177.97 ± 0.10	100.77	139.23
47.6	0	177.79 ± 0.21	100.97	139.03
50 a)	1	178.06 ± 0.13	100.91	139.09
57.44	0	178.02 ± 0.14	100.83	139.17
59.22	1	178.00 ± 0.19	100.99	139.01
66 a)	1	178.04 ± 0.10	100.87	139.13
75 a)	1	177.99 ± 0.12	100.64	139.36
85 a)	0	178.26 ± 0.12	100.76	139.24

a) poorly separated resonances; the spin of the dominating resonance is taken into account.

b) statistical error

fragment mass- and energy-distributions were obtained as a function of neutron energy. With the same apparatus, also the spontaneous fission of ^{240}Pu was measured during a one month stop of LINAC. The average pre-neutron emission total kinetic energy is found to be (0.8 ± 0.3) MeV higher for the thermal neutron induced fission of ^{239}Pu than for the spontaneous fission of ^{240}Pu. The mass-distribution for both fissioning systems are similar. However, the fine-structure is more pronounced, the peak-to-valley ratio is larger and the peaks are narrower for the spontaneous fission. In the neutron resonance region we only observe small fluctuations in the average total kinetic energy $\bar{E}_K$ for the 0^+ and the 1^+ resonances. This is discussed in terms of the channel theory of fission. Results are shown in Fig. 1.1.3. and Table 1.1.1. The work has been presented at the International Symposium on Physics and Chemistry of Fission, Jülich, 14-18 May 1979.

Identifications of s- and p-wave contributions to intermediate structure in the capture cross section of ^{238}U

M.S. Moore, F. Corvi, L. Mewissen, F. Poortmans

Intermediate structure has recently been reported by Perez et al. [1] in the radiative capture cross section of ^{238}U for neutron energies between 5 and 100 keV. In their analysis, Perez et al. assumed that this structure is due to p 3/2 doorway states in the entrance channel. It is of interest to verify this assumption and to check the consistency of the proposed interpretation by comparing the observed density of intermediate structure levels with a calculation of the doorway-state density. We have carried out a preliminary measurement to identify the relative s- and p-wave contributions to this structure by using the high bias - low bias technique devised by Corvi et al. [2]. This technique involves comparing the contribution of the highest energy primary gamma transitions (characteristic of p-wave neutrons) with all transitions. To permit an assessment of statistical accuracy, we introduced an intermediate bias window with roughly the same counting statistics as the high-bias window but with no s- to p-wave discrimination. As a measure of the intermediate structure, we took the ratio of the observed count rate in ~ 400 eV wide bins to the count rate in a running average centered around the same bin but 4400 eV wide. This quantity showed clearly the intermediate structure fluctuations reported by Perez et al. We then calculated the correlation coefficients of the various windows, finding that the control (intermediate-bias) window showed a significant correlation ($r = 0.49$ with 33 degrees of freedom) while the high-bias window gave no significant correlation ($r = 0.12$) for the structure below 20 keV. This suggests that the intermediate structure is either due to s-wave neutrons or is due to special transitions that do not populate the lowest levels in ^{239}U. We plan additional measurements with improved statistical accuracy to confirm these preliminary results and to extend the range to 100 keV.

Fission cross-section of ^{235}U

C. Wagemans, R. Barthélémy

(WRENDA 76/77: 739, 748)

A detailed report on the fission cross-section measurements in the neutron energy region from thermal up to 30 keV was presented at the Conference on Nuclear Cross Sections and Technology [3].

Fig. 1.1.4. shows the $\sigma_f(E)\sqrt{E}$-data between 0.02 and 1 eV neutron energy as obtained from these measurements. Another result of these measurements is the value of 247 ± 3 barn.eV for the fission integral from 7.8 to 11 eV, which is often used for normalization purposes. This value agrees with the latest data published by Czirr and Carlson [4] and by Gwin et al. [5].

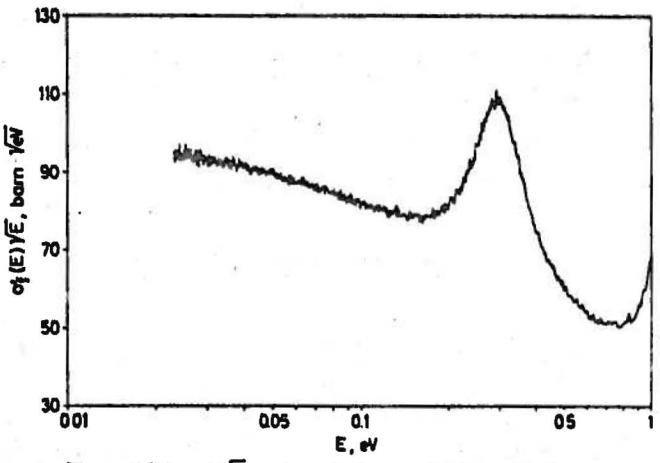

Figure 1.1.4 $\sigma_f\sqrt{E}$-values between 0.02 and 1eV

Measurement of the neutron induced capture cross section and α of ^{235}U between 1 and 100 keV

L. Calabretta*, F. Corvi, M. Merla

(WRENDA 76/77: 721, 726, 727, 755)

An experiment was set up to measure both the ^{235}U capture cross section and α, the capture-to-fission ratio, in the keV region. The sample consisted of a multi-plate fission chamber operated with continuous methane flow at atmospheric pressure. The chamber characteristics are given in Table 1.1.2. The efficiency ϵ was determined by measuring the ratio of coincidences to singles in a fast neutron detector viewing the chamber. A preliminary run was performed last September on a 28 m flight path. A resolution of 0.5 ns/m was obtained when running the linac at maximum power and using the rotary uranium target. The sample was viewed by two C_6F_6 scintillators of 10.2 cm diameter and 7.6 cm height: those pulses in coincidence with the fission chamber pulses were considered to be due to fission γ-rays. Normalization of the capture yield was performed with a gold sample (0.6 mm thick), applying the usual weighting method. Such a preliminary run showed the feasibility of the method; typically a one-to-one signal-to-background ratio was observed for the capture yield at 30 keV, using unshielded detectors. However the data collected were not considered sufficient for an investigation of the detailed structure of capture and

* E.C. Bursary.

TABLE 1.1.2

Description of the Fission Chamber

Number of aluminium plates	22
Thickness of aluminium plates	30 μ
Thickness of end windows	50 μ
Diameter of back-to-back U_3O_8 coatings	9.0 cm
Average thickness of coatings	1.18 mg/cm^2
^{235}U enrichment	99.508 %
Total mass of ^{235}U	2.678 g
Average plate spacing	0.2 cm
Efficiency	85 %

fission cross sections. A longer run is planned for the next year using four C_6F_6 detectors to improve the statistics.

1.1.2 *Structural Materials*

Total Neutron Cross Section Measurements on ^{54}Fe, ^{56}Fe and ^{57}Fe

E. Cornelis, C.R. Jungmann, L. Mewissen, F. Poortmans

(WRENDA 76/77: 167)

High resolution total neutron cross section measurements have been performed on samples of enriched isotopes (on loan from ORNL) of ^{54}Fe, ^{56}Fe and ^{57}Fe in the energy range from 35 keV up to 2 MeV. The experiments were made on a 200 meter flight path at the LINAC using a plastic scintillator (NE 110) as neutron detector. The R-matrix multi-level code FANAL [6] was used to fit the broad s-wave resonances and the multi-level Breit-Wigner code SIOB [7] to fit the narrow $l > 0$ resonances. The analysis is completed for ^{54}Fe and ^{56}Fe up to a neutron energy of 300 keV.

Neutron Capture Cross Section of ^{56}Fe in the range 1 - 100 keV

A. Brusegan, F. Corvi, G. Rohr, R. Shelley, T. van der Veen

(WRENDA 76/77: 184 - 196)

The measurements were performed at a 60 m flight-path station at the Geel linear electron accelerator operated at 4ns burst width and 800 hertz repetition frequency. The capture detectors consisted of two deuterated benzene (C_6D_6) liquid scintillators encapsulated in thin aluminium containers of 10.2 cm diameter and 7.6 cm height. The sample, on loan from ORNL, consisted of iron oxide enriched to 99.93 % ^{56}Fe, packed

in an aluminium container of 8 cm diameter and 0.3 mm thick wall. The sample thickness was 0.015 atoms/barn.
The capture events were weighted according to their measured pulse height to achieve a detector response proportional to the total energy released in the capture process. A part of this "weighted" time-of-flight spectrum is plotted in Fig. 1.1.5. Data were

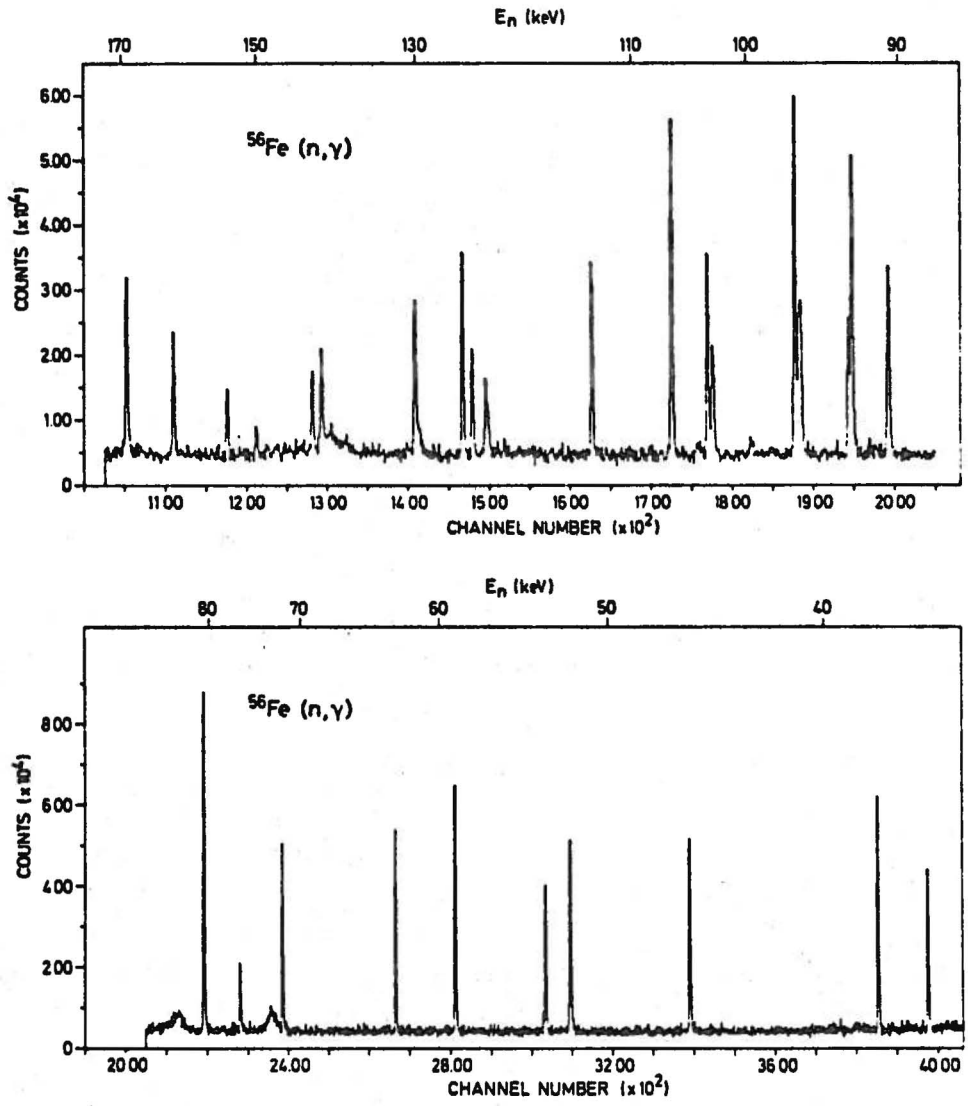

Figure 1.1.5

recorded in the neutron energy range 0.5 - 600 keV but the analysis was completed only up to 100 keV. The energy dependence of the neutron flux was measured with a 0.5 mm thick Li-glass detector. Special effort was put into the normalization of the capture data: first, a transmission measurement was performed in order to deduce precise parameters of the 1.15 keV resonance. The value $\Gamma_n = 58 \pm 4$ meV was found for its neutron width, in agreement with the value $\Gamma_n = 56 \pm 6$ meV deduced from normalizing the capture data at thermal energy.

The capture data normalized to the area of the 1.15 keV resonance, assuming Γ_n = 58 meV, are listed in Table 1.1.3 together with the Perey [8] evaluation and the Harwell [9] preliminary data. The resonance parameters were deduced from the capture areas using a modified version of the TACASI code. A comparison with the results given in refs. (8) and (9) shows that the present capture areas are on the average 8 % larger than Harwell's preliminary results but 15 % lower than the Oak Ridge values.

TABLE 1.1.3

Resonance parameters of ^{56}Fe between 1 and 100 keV

	PRESENT RESULTS				OAK RIDGE EVALUATION			HARWELL
E_0 (keV)	$g\Gamma_n\Gamma_\gamma/\Gamma$ (eV)	Γ_n (eV)	Γ_γ (eV)	$g\Gamma_n\Gamma_\gamma/\Gamma$ (eV)(a)	Γ_n (eV)	Γ_γ (eV)	J l	$g\Gamma_n\Gamma_\gamma/\Gamma$ (eV)(b)
1.152	(53. ± 4.)x10^{-3}	(58. ± 4.)x10^{-3}		(53. ± 3.8)x10^{-3}	(60. ± 4.)x10^{-3}	0.6 ±0.06	1/2 1	(4.9 ±1)x10^{-3}
2.352	(0.54 ± 0.1)x10^{-3}	(0.27 ± 0.05)x10^{-3}		(0.4 ± 0.12)x10^{-3}	(0.2 ± 0.06)x10^{-3}	0.84	3/2 2	(0.39±0.03)x10^{-3}
12.46	(2.3 ± 0.4)x10^{-3}	(2,3 ± 0.4)x10^{-3}		2.3 x 10^{-3}	(2.3 ± 0.3)x10^{-3}	0.54	1/2 1	(2.8 ±0.7)x10^{-3}
17.76	(17. ± 2,)x10^{-3}	(17. ± 2.)x10^{-3}		19. x 10^{-3}	(19. ± 2.)x10^{-3}	0.54	1/2 1	(14.5 ±1.3)x10^{-3}
20.18	(7.8 ± 1.2)x10^{-3}	(3.9 ± 0.6)x10^{-3}		9.4 x 10^{-3}	(4.7 ± 0.5)x10^{-3}	0.84	3/2 2	(5.1 ±2.8)x10^{-3}
22.80	0.17 ± 0.03	0.24 ± 0.04		0.18	0.27 ± 0,06	0.54	1/2 1	0.15±0.04
27.68	0.80 ± 0.20		0.80±0.20		1520 ± 30.	1.4 ±0.1	1/2 0	0.86±0.02
34.24	0.54 ± 0.08		0.46±0.08	0.64 ± 0.05	0.79 ± 0.3	0.54	3/2 1	0.44±0.01
36.73	0.23 ± 0.03	0.086 ± 0.01		0.28 ± 0.02	0.11 ± 0.01	0.84	5/2 2	
38.42	0.34 ± 0.05	0.25 ± 0.035		0.4	0.32 ± 0.08	0.54	3/2 1	
46.06	0.45 ± 0.06		0.48±0.06	0.5	10.0 ± 3.0	0.53±0.05	1/2 1	
52.14	0.68 ± 0.08		0.35±0.04	0.81	12.0 ± 1.0	0.42±0.04	1/2 1	
53.57	0.33 ± 0.07		0.51±0.09	0.4	1.0 ± 0.4	0.67±0.17	1/2 1	
53.70	0.032 ± 0.01	0.034 ± 0.01						
59.23	0.74 ± 0.1		0.42±0.05	0.87	4.0 ± 0.5	0.49±0.05	3/2 1	
63.47	0.55 ± 0.1		0.41±0.075	0.65	0.8 ± 0.16	0.55±0.13	3/2 1	
72.98	0.61 ± 0.09		0.62±0.09	0.7	20. ± 4.	0.72±0.07	1/2 1	
74.00	0.57 ± 0.07		0.57±0.07	0.73	535. ± 10.	0.73±0.07	1/2 0	
77.07	0.27 ± 0.04		0.29±0.04	0.3	3.6 ± 0.5	0.33±0.03	1/2 1	
80.84	1.75 ± 0.2		0.63±0.085	2.04	7.0 ± 0.7	0.74±0.08	5/2 2	
83.69	0.50 ± 0.20		0.50±0.20	1.28	1250. ± 50.	1.28±0.13	1/2 0	
90.33	0.73 ± 0.1		0.37±0.05	0.89	14. ± 1.	0.46±0.05	3/2 1	
92.70	0.93 ± 0.2		0.66±0.12	0.93	1.6 ± 0.3	0.65±0.11	3/2 2	
92.93	0.40 ± 0.1	0.32 ± 0.08		0.53	0.52 ± 0.15	0.54	3/2 1	
96.22	0.55 ± 0.2	0.22 ± 0.08		1.26	0.67 ± 0.40	1.1 ±0.9	5/2 2	
96.37	0.38 ± 0.1		0.51±0.15	0.3	1.3 ± 1.1	0.4 ±0.3	1/2 1	
96.62	1.06 ± 0.2		0.68±0,12	0.7	2.5 ± 0.3	0.4 ±0.2	3/2 1	

a) 10% error unless given

b) Γ_γ assumed to be 1 eV

^{54}Fe(n,α)^{51}Cr and ^{54}Fe(n,p)^{54}Mn Cross Section Measurements by Activation Techniques

A. Paulsen, R. Widera, F. Arnotte, H. Liskien

(WRENDA 76/77: 205-207)

Helium produced via (n,x α) reactions contributes to the embrittlement of fast reactor structural materials. Cross sections of (n,α) reactions on the main constituents of stainless steel, namely Cr, Fe and Ni, are therefore important in this context. Since these reactions lead in most cases to stable product nuclei, and a corresponding measuring programme for elemental (n,α) cross sections using direct α-particle detection is running in our laboratory, cross sections for the reaction ^{54}Fe(n,α)^{51}Cr can supplement the data to be expected. The half-life of 27.75 d and the emitted gamma-

radiation of 320 keV in 9.815 % of the decaying ^{51}Cr product nuclei mean that these cross sections may be measured by activation techniques. When these cross sections are known much better than at present, the reaction $^{54}Fe(n,\alpha)^{51}Cr$ could also be of interest for dosimetry purposes via foil activation. Iron foils are often used in dosimetric activation measurements via the $^{56}Fe(n,p)^{56}Mn$ and $^{54}Fe(n,p)^{54}Mn$ reactions, so that the possibility of extracting additional information from the induced ^{51}Cr activity in the same sample foil will be attractive.
Ratios of cross sections for the reactions $^{54}Fe(n,\alpha)^{51}Cr$, $^{54}Fe(n,p)^{54}Mn$ and $^{56}Fe(n,p)^{56}Mn$ were measured by activation techniques. In the 6 to 10 MeV energy range quasi-monoenergetic neutrons produced by the D(d,n) source reaction were used, while additional data were obtained between 12 and 17 MeV using the T(d,n) source reaction. The cross section ratios have accuracies between 1.5 and 4.5 %. For comparison with available cross section data the measured cross section ratios were converted to absolute scale ^{54}Fe cross sections by multiplication with some reference cross sections. Fig. 1.1.6. shows a plot of the $^{54}Fe(n,p)$ and $^{54}Fe(n,\alpha)$ results together with existing

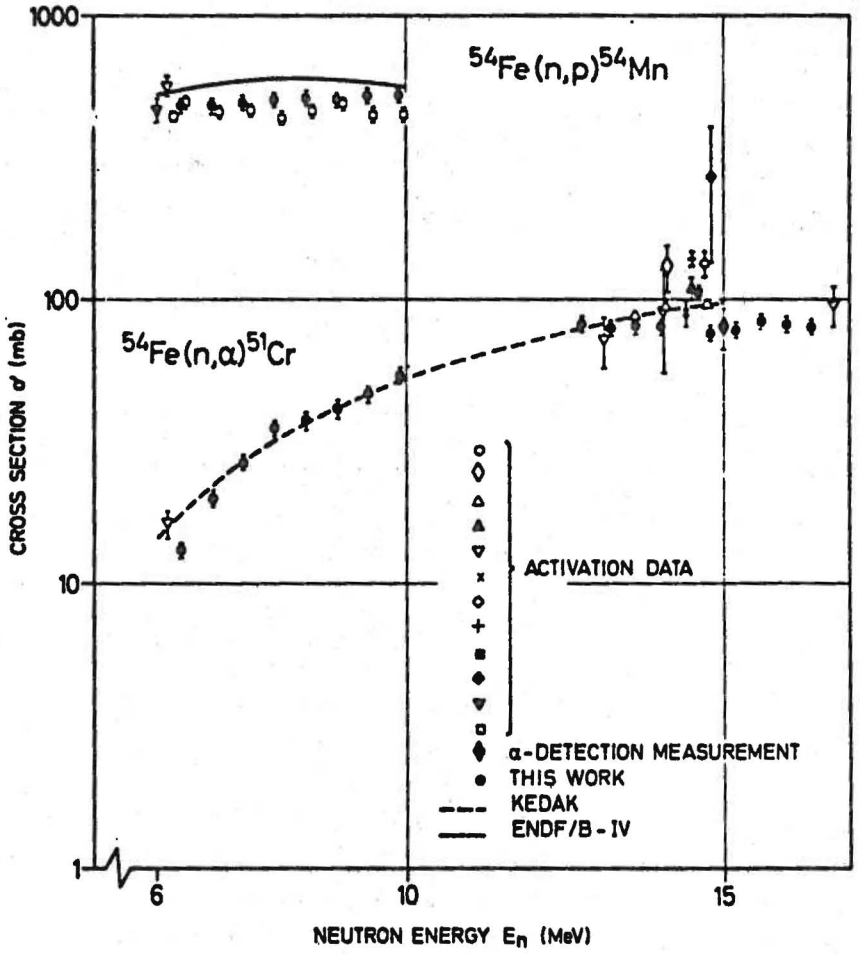

Figure 1.1.6 Comparison of the results with existing cross section data above 6 MeV for the reaction $^{54}Fe(n,\alpha)^{51}Cr$ and between 6 and 10 MeV for the reaction $^{54}Fe(n,p)^{54}Mn$.

data. The scatter of existing $^{54}Fe(n,\alpha)$ data at 14 MeV is large and the present results support the lower values. Our results are in excellent agreement with the results of the only direct α-particle detection measurement at 15 MeV. This result must also include possible $(n,n\,\alpha)$ and $(n,\alpha n)$ contributions which are obviously small. All the other measurements are activation measurements identifying the product nuclei by half-life and characteristic radiation. Deviating assumptions about the gamma-emission probability can only partly explain the discrepancies. The present results support the KEDAK data in the 6 to 13 MeV range. For the $^{54}Fe(n,p)^{54}Mn$ results there is reasonable agreement with all existing data but a rather strong discrepancy with the ENDF/B-IV data.
A paper for publication is submitted to Nucl. Sci. Eng. [10].

Measurement of (n,α) Cross Sections on Cr, Fe and Ni in the 5 to 10 MeV Neutron Energy Range

A. Paulsen, H. Liskien, F. Arnotte, R. Widera

(WRENDA 76/77: 245 - 248)

Helium formed in stainless steel through (n,α) reactions influences the mechanical and dimensional properties of nuclear reactor structures. For thermal reactors this helium formation is mainly governed by the two-step process $^{58}Ni(n,\gamma)^{58}Ni(n,\alpha)^{56}Fe$, but for fast reactors the (n,α) reactions on the constituents of stailess steel are dominant [11]. Cross section measurements for these (n,α) reactions have been carried out in very few cases at 14 MeV neutron energy. Therefore the measurement of elemental (n,α) cross sections of Cr, Fe and Ni is requested by the designers of fast reactors in the neutron energy range from threshold (~ 5 MeV) to 15 MeV.
As the (n,α) reactions on the involved main isotopes are leading to stable or very long living (^{56}Fe) nuclei the activation techniques are not applicable. To study the elemental (n,α) cross sections of Ni, Fe and Cr we designed a reaction chamber for direct α-particle detection during neutron irradiation at the 7 MV electrostatic accelerator of the CBNM. A cross section view of this chamber is shown in Fig. 1.1.7. Five telescopic charged particle detectors, each consisting of two energy loss detectors (proportional counters) and one remaining energy detector (surface barrier counters) in a triple-coincidence arrangement, are registering the charged particles emitted from a thin metallic foil (about 3 mg/cm^2) in the center of the chamber. The mean observation angles relative to the incoming neutron beam are 14, 51, 79, 109 and 141°. All the energy loss detectors are combined in two pairs of proportional counters, one pair on each side of the sample. A neutron collimator is used between neutron source and reaction chamber to keep random coincidences at an acceptable level and to suppress neutron-induced charged particle production in the surface barrier counters. In the middle of the chamber a movable slide permits to insert different samples (the sample to be studied, a reference sample, a background position and a radioactive α-source).

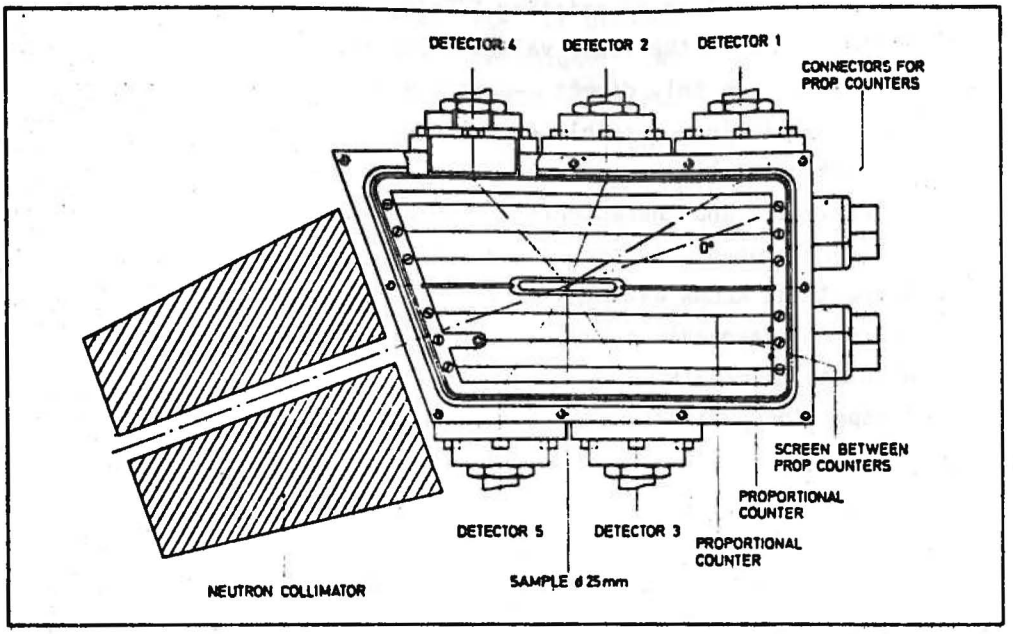

Figure 1.1.7 Cross-section view of reaction chamber and neutron collimator.

The electronics of this chamber are sketched in Fig. 1.1.8. After extraction of the timing information by the indicated threshold discriminators the analogue signals

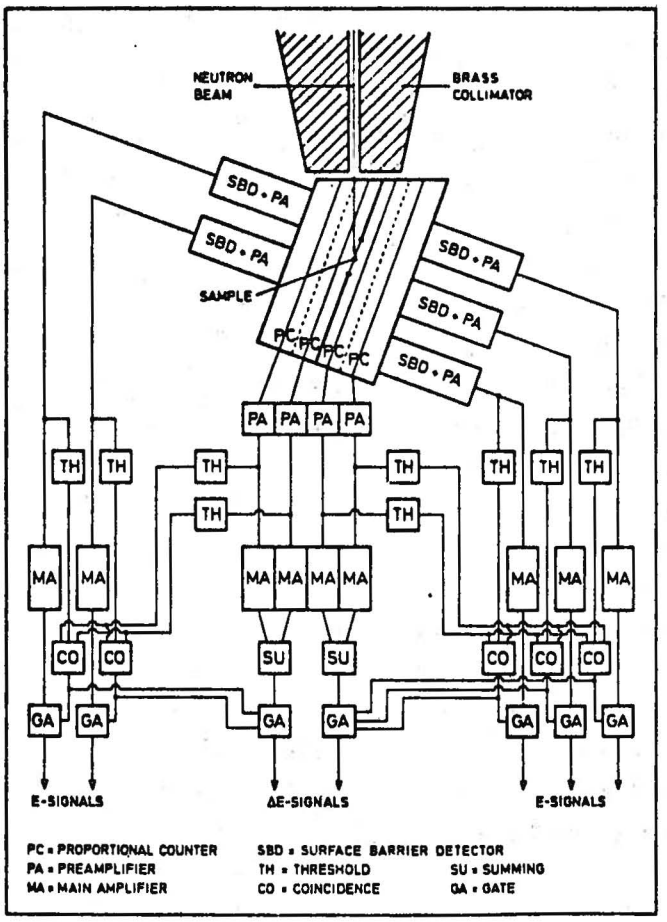

Figure 1.1.8 Experimental set-up for reaction chamber.

from each pair of proportional counters are summed and led together with the five E-signals to the multi-parameter data acquisition system (ND 6600) which serves in this case as a fivefold bi-parametric analyser.
Fig. 1.1.9 indicates the measuring procedure. The differential (n,α) cross sections

Evaluation of differential cross sections from measured

reaction rates $R_i^{n,\alpha} = \phi_n \cdot N \cdot \left(\frac{d\sigma}{d\Omega}\right)_i^{n,\alpha} \cdot \Omega_n \cdot \Omega_i$, i = 1 to 5

$$\left(\frac{d\sigma}{d\Omega}\right)_i^{n,\alpha} = \frac{R_i^{n,\alpha}}{\phi_n \cdot N \cdot \Omega_n \cdot \Omega_i}$$

ϕ_n : neutrons/sr · s

N : nuclei/cm²

as a similar equation is valid for $\left(\frac{d\sigma}{d\Omega}\right)_1^{n,p}$ of the elastic n-p scattering

$$\phi_n = \frac{R_1^{n,p}}{\left(\frac{d\sigma}{d\Omega}\right)_1^{n,p} \cdot P \cdot \Omega_n \cdot \Omega_1}$$

P : H nuclei/cm²

$$\Longrightarrow \left(\frac{d\sigma}{d\Omega}\right)_i^{n,\alpha} = \left(\frac{d\sigma}{d\Omega}\right)_1^{n,p} \frac{R_i^{n,\alpha} \cdot P \cdot \Omega_1}{R_1^{n,p} \cdot N \cdot \Omega_i}$$

Figure 1.1.9 Measuring procedure.

for the five observation angles are calculated from the observed reaction rates. Since the information about the neutron flux is deduced from a measurement of the recoil proton scattering rate from a polyethylen foil into detector 1 (about 14° observation angle) the final differential cross sections are directly proportional to the assumed differential n-p scattering cross section. Besides the reaction rates and foil characteristics the result depends furtheron in a good approximation only on the ratios of the detector solid angles which are measured with an ^{241}Am α-source. The dynamic range of the used electronics is insufficient to record simultaneously the spectra of emitted protons and α-particles. Consequently the recoil protons are observed in a separate run. Since the used deuterium gas target for the D(d,n) neutron source is very stable in time the beam charge integrator serves as a neutron monitor linking the runs.
For nickel and iron results are available whereas the measurements on chromium are running. The hyperbola-like curved α-mountain is clearly identified in the bi-parametric (E,ΔE) pulse height spectra of the five detectors. An integration over the ΔE-axis and correction for energy losses in the sample foil and counter gas yields rather clean α-spectra which are shown in Fig. 1.1.10 for nickel and 79° observation angle and which are similar for iron.
These spectra can be well fitted with a so-called compound nucleus evaporation shape. The constant low-energy boundary is due to the Coulomb barrier of the separating

nuclei and the high-energy boundary increases with increasing neutron energy, according to the increase of energy available to the reaction. The determination of average Q-values through average α-energies permitted the transformation of the angular distributions into the center-of-mass system. Fig. 1.1.11 shows some of the Ni c.m. angular distributions. Figs. 1.1.12 and 1.1.13 show the relative fitting coefficients for Legendre polynomials up to the second order for the Ni and Fe c.m. angular distributions respectively. Values of A_1/A_0 are roughly zero and values of A_2/A_0 are decreasing with increasing neutron energy. Both statements are in qualitative agreement with the expectations from a reaction model of the compound nucleus theory. The data points shown around 14 MeV refer to $^{58}Ni(n,\alpha)$ measurements of Seebeck and Bormann [12] and Khan et al. [13] with the isotropic $^{58}Ni(n,n\,\alpha)$ contribution subtracted and to the $^{56}Fe(n,\alpha)$ measurement of Dolya et al. [14] assuming a negligible $^{56}Fe(n,n\,\alpha)$ contribution.

The resulting angle-integrated $Ni(n,\alpha)$ cross sections are shown in Fig. 1.1.14. The two existing data points for elemental nickel are a quadrupole spectrometer measurement at 15 MeV from Livermore [15] and a high sensitivity gas mass spectrometer measurement at 14.8 MeV of Farrar IV. and Kneff [16]. All results are in reasonable agree-

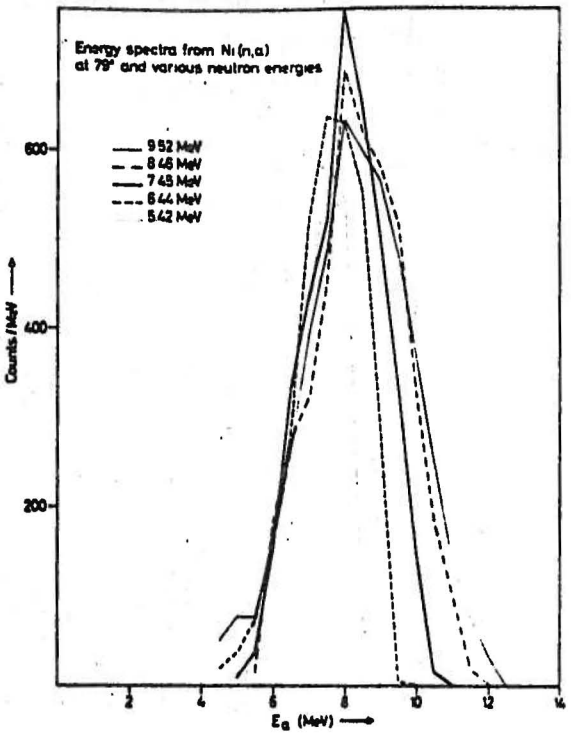

Figure 1.1.10

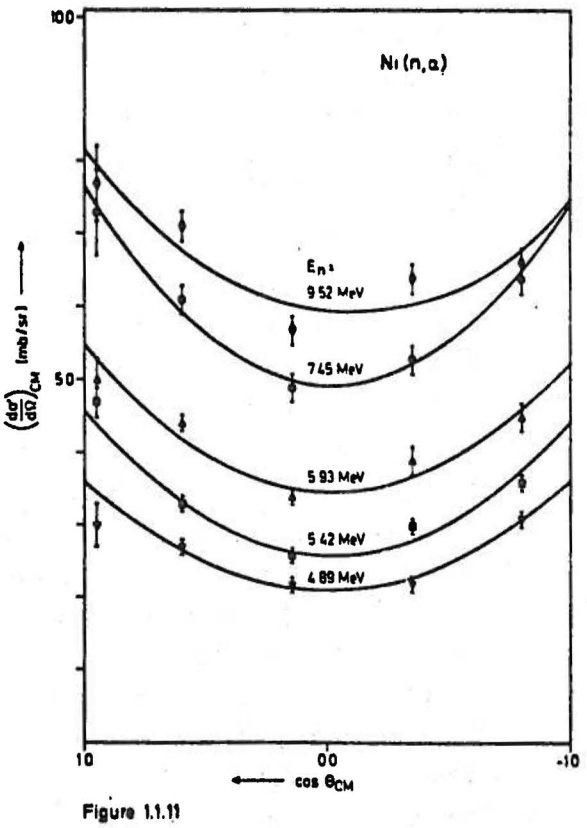

Figure 1.1.11

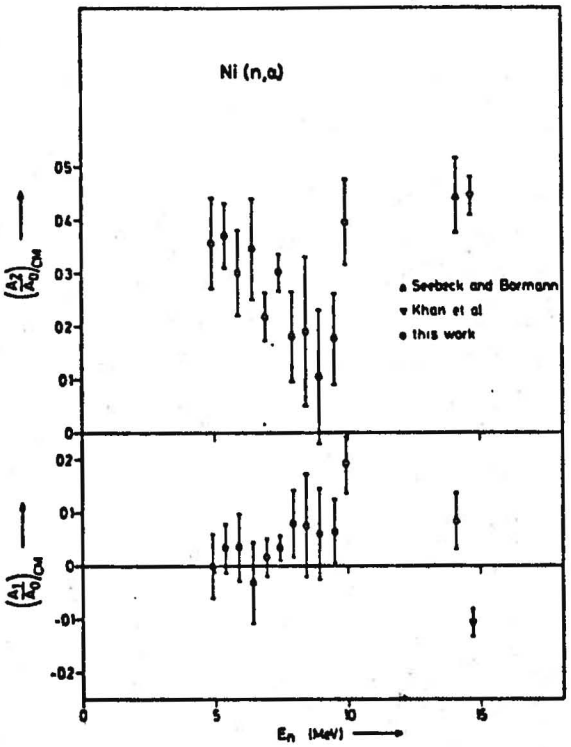

Figure 1.1.12

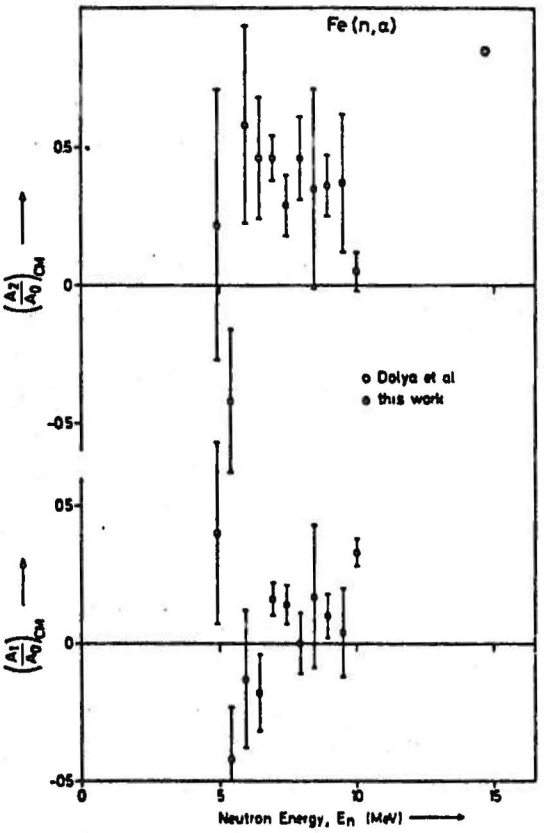

Figure 1.1.13

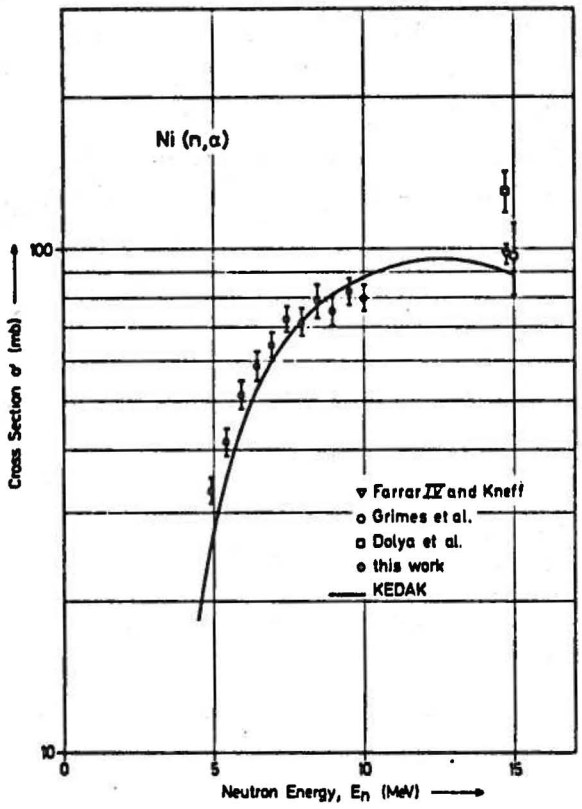

Figure 1.1.14

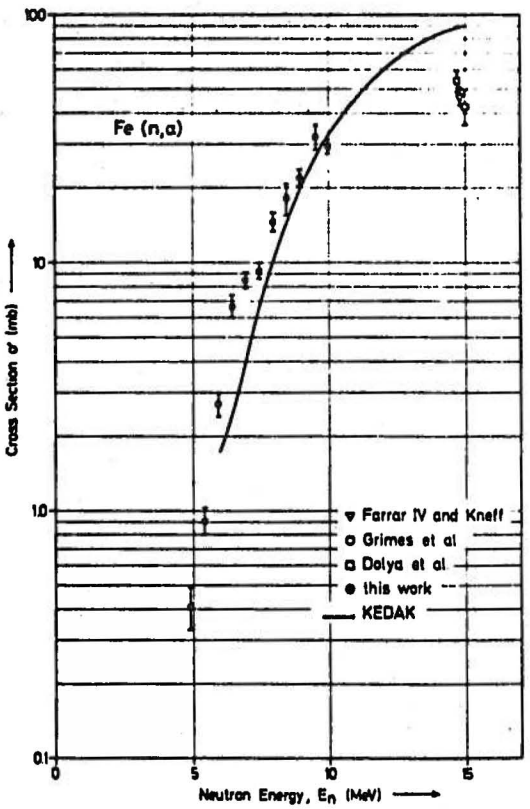

Figure 1.1.15

ment with a cross section curve constructed from the KEDAK data file and which is based on theoretical model calculations having the $^{58}Ni(n,\alpha)$ contribution normalized to a 14 MeV measurement. A measurement on ^{58}Ni, ^{60}Ni and ^{62}Ni at 14.7 MeV by Dolya et al. [14] results in 131 ± 13 mb for natural nickel and is considerably higher than the elemental nickel results.
The corresponding Fe(n,α) results are shown in Fig. 1.1.15. Again the two existing data points around 15 MeV for elemental iron of Grimes et al. [15] and Farrar IV and Kneff [16] are in good agreement. But these results are also in reasonable agreement with the result of Dolya et al. [14] which adds up to 54 ± 5 mb at 14.7 MeV from measurements on the isotopes ^{54}Fe, ^{56}Fe, ^{57}Fe and ^{58}Fe. The cross section curve constructed from the KEDAK data file is again based on theoretical model calculations having only the very small contributions from ^{54}Fe and ^{58}Fe normalized to experimental 14 MeV values. This curve is in a rather rough agreement with the results of this work, but it is about a factor of two higher than the experimental results around 15 MeV.

High resolution transmission experiments on Sulphur

C.R. Jungmann, E. Cornelis, L. Mewissen, F. Poortmans, H. Weigmann

Two series of transmission experiments were performed on a natural sulphur sample (95 % of ^{32}S). The first experiment was performed on a 200 meter flight path of the Linac facility, using a moderated neutron beam and covering the energy range from 100 keV up to 2 MeV. A second series of measurements, in the neutron-energy range from 250 keV up to 15 MeV, was done on a 400 meter flight path and using the direct beam from the neutron-producing uranium target. In both experiments, the burst and channel widths were 4 nsec. Fig. 1.1.16 shows the experimental total cross section for sulphur in the energy range from 0.5 MeV up to 1.5 MeV taken at the 400 meter flight station (resolution 0.01 nsec/meter).
One of the aims of these measurements is to look in (^{32}S + n) for possible isobaric analog states of low lying states in ^{33}P. The analysis of the data is in progress.

1.1.3 *Fission Products*

Resonance Parameters of Pd Isotopes

P. Staveloz, E. Cornelis, L. Mewissen, F. Poortmans, G. Rohr, R. Shelley, T. van der Veen

(WRENDA 76/77: 405, 406)

The cross section experiments on the stable Palladium isotopes (on loan from Oak Ridge National Laboratory) are nearly completed and an important part of the data has been analyzed. Resonance parameters are deduced from total, elastic scattering and capture cross section experiments performed at the neutron time-of-flight spectrometer of the

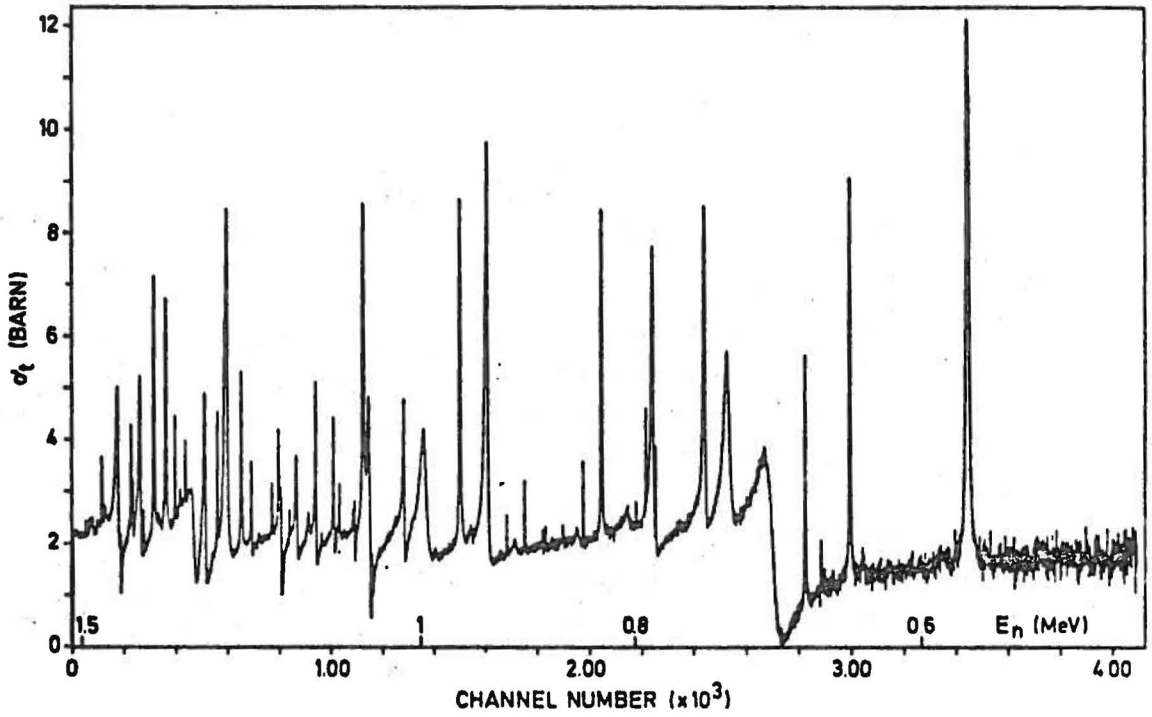

Figure 1.1.16 Experimental total cross section for sulphur in the energy range from 0.5 MeV up to 1.5 MeV taken at the 400 meter flight station (resolution 0.01 nsec/meter).

150 MeV Linac of CBNM. Parity assignments are made on the basis of low bias to high bias ratios deduced from capture gamma ray spectra. The resonance parameter analysis is completed for ^{105}Pd and partial results are available for the even isotopes ^{104,106,108,110}Pd.

For ^{105}Pd, neutron widths were determined for 200 resonances and the capture widths for 71 of them. The final results are:

Average Capture Width: $\langle \Gamma_\gamma \rangle = 150$ meV $\pm$ 1 meV (stat. error)
$\pm$ 8 meV (syst. error)

s-wave Strength Function: $S_0 = \frac{\Sigma\, g\Gamma_n^0}{\Delta E} = (0.63 \pm 0.07) \times 10^{-4}$

The level spacing has been determined using a method which separates large s-wave resonances from smaller ones and from resonances with higher angular momentum ($l \geq 1$) by means of the Bayes theorem. The number of s-wave resonances lost in this procedure has been estimated assuming a Porter Thomas distribution of the reduced

neutron widths. For ^{105}Pd this yields a value of:

$$D = (10.0 \pm 0.5)\ eV.$$

The work for the even Pd isotopes is not completed yet but preliminary results show very pronounced intermediate structure effects in the strength functions.

1.1.4 *Miscellaneous*

Neutron Spectra from (α,n) reactions
G. Jacobs, H. Liskien

A neutron detector system based on NE 213 liquid scintillation has been set up. It delivers three signals: the neutron time-of-flight (TOF), a signal proportional to the scintillation light (PHE) and a pulse shape signal (PSA). These three signals are stored, event for event, in a data acquisition and processing system ND 6660. A neutron energy range from 0.2 to 20 MeV is covered. The derivation of the PSA-signal can occur using different electronic systems. Most promising are LINK 5010, ORTEC 552 and CANBERRA 2160. Advantages and disadvantages are such that an experimental intercomparison is indispensable. A block diagramme of the detection system using the LINK 5010 unit as a pulse shape analyser is given in Fig. 1.1.17.

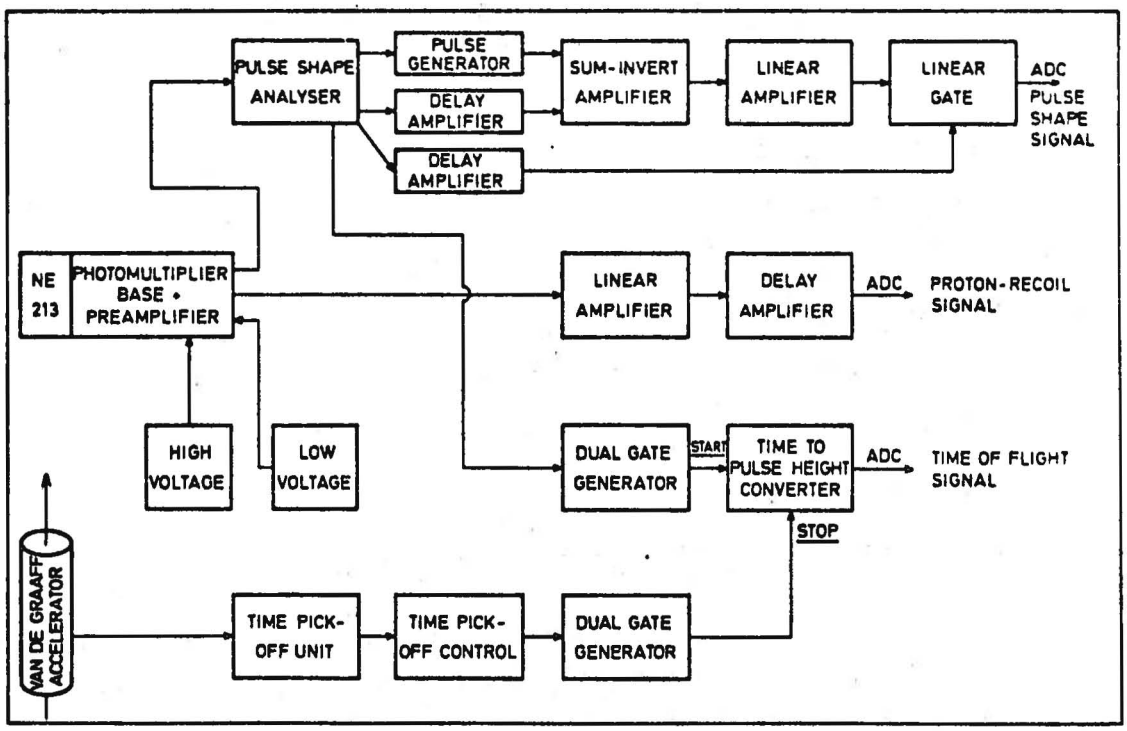

Figure 1.1.17 Schematic drawing of the detection system using the "LINK 5010" pulse shape analyser.

Tritium production cross sections of Al and Nb
H. Liskien

Irradiations of high purity aluminium and niobium samples were performed using the CN Van de Graaff accelerator which produced neutrons in the 15 - 20 MeV neutron energy range. The samples were analysed at KFA JÜlich using gas extraction and tritium gas counting. The results are only partially of value due to small tritium cross-contamination between T-Ti targets used for neutron production and the irradiated sample.

(n,p) and (n,α) cross sections of ^{23}Na
H. Weigmann, G.F. Auchampaugh, G.L. Morgan
Collaboration: LASL.

^{23}Na is a favourable case to study in detail the physical origin of the structures observed in many (n,p) and (n,α) cross sections of light and medium nuclei. Measurements have been done in the neutron energy range from threshold to ~ 10 MeV, using the WNR facility of LASL. Analysis of the data is in progress.

(n,p) and (n,α) cross sections of ^{40}K in the resonance region
C. Wagemans, H. Weigmann, R. Barthélémy
Collaboration: SCK-CEN/Mol.

The $^{40}K(n,\alpha)$ and $^{40}K(n,p)$ cross sections were measured in the neutron energy region 0.02 eV to 70 keV. The protons and the alpha particles were detected with a large surface barrier detector at a 9.4 meter flight-path of GELINA. The reaction cross sections show a pronounced resonance structure with a mean level spacing of about 1.5 keV. In contrast to the thermal neutron region, where about ten times more (n,p) than (n,α)-reactions are observed, most of the resonances are due to (n,α)-processes. Further analysis of the data with respect to resonance parameters is in progress.

1.1.5 *Major Research Equipment*

Improvements at the LINAC
R. Cools, R. Forni, F. Massardier, F. Menu, K. Meynants, J.M. Salomé, P. Siméone, F. Van Reeth, J. Waelbers, C. Waller

Operation of the Linac was interrupted in April 1979 for the installation of a rotary target (Fig. 1.1.18). This target consists of a mercury cooled uranium torus. The high current for driving the electromagnetic pump is transferred to the rotary part of the system by big sliding contacts. The new installation was checked up to 9.5 kW electron beam power. The temperature of the uranium was 200°C at the enter of the beam and 150°C at the canning. This is to be compared with 600°C and 300°C respectively in the stationary target at 5 kW. This new type of target therefore can easily cope with the maximum beam power available from the Linac. The stationary and the rotary uranium targets were used alternatively during the second part of the year

for neutron measurements according to the experimental requirements. A beam power of 9 kW was injected into the new rotary target during 622h. Polyethylene moderators cannot be used at this beam power level due to the very high gamma heating and radiation damage. A new moderator consisting of water filled beryllium boxes of 2 mm wall thickness has been built and works satisfactorily. Two such boxes were installed above and below the target. They are interconnected by means of two small pipes to avoid bubbles in the lov r box. The water temperature is controlled by the elongation of a stainless steel bellow connected to the moderators.

A large cathode electron gun was tested in the laboratory. An emitted current up to 45A was measured at the beam cross-over.

The study of the post acceleration bunching system was continued. The energy spectra of the electron micro-bunches have been calculated and compared with the results of preliminary measurements. The agreement is reasonable. Following these studies a pulse compression factor of 3.3 seems to be realistic. These studies also indicated that the bunching system can be made more effective if some improvements at the

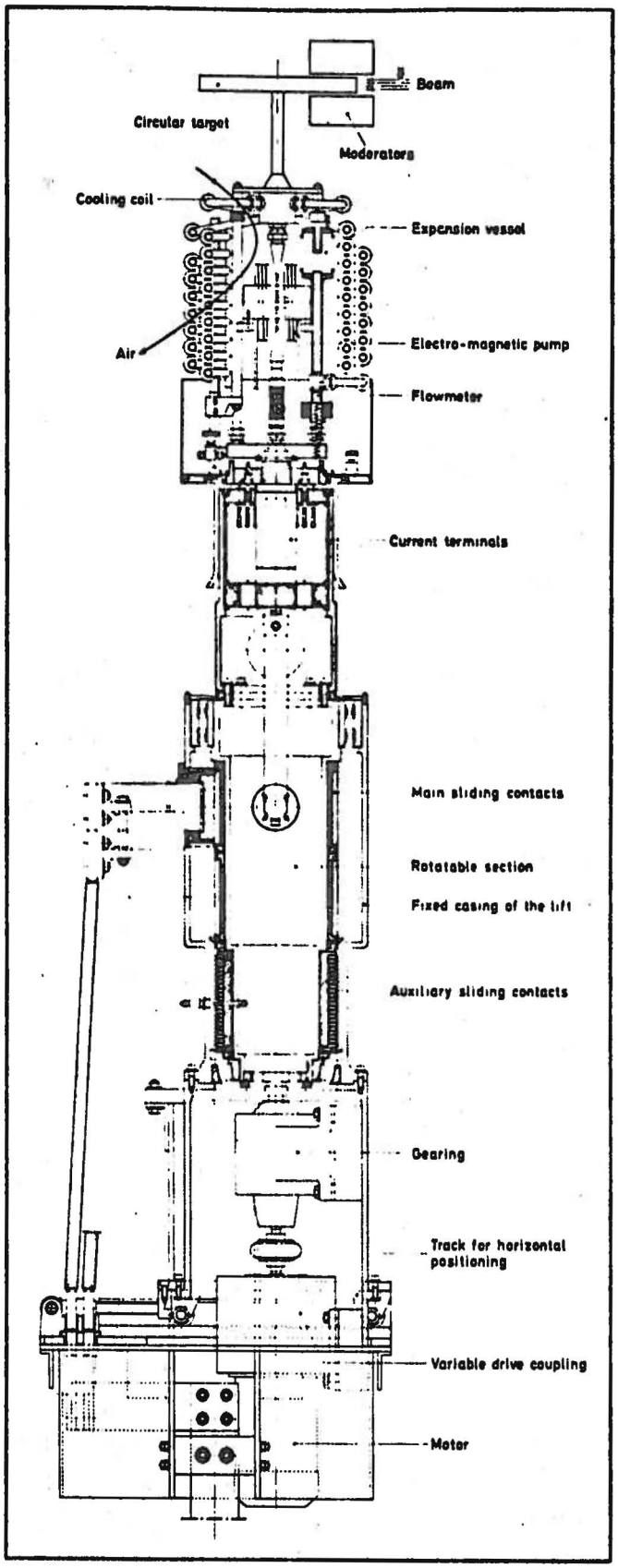

Figure 1.1.18

injection side (magnetic field at the electron gun, displacement of the pre-bunching cavity) are realised.

Improvement of the CN-7 MV Van de Graaff

A. Crametz, P. Falque, J. Leonard, R. Smets

At the beginning of May, a DC deuteron beam of 3 MeV of 50 μA on the target was obtained (the guaranteed DC proton beam performance is 35 μA) for a two days irradiation experiment in co-operation with the Kernforschungsanlage JÜlich.
A third beam line at the 45° right output of the switching magnet was fully installed and is in operation since October.
With the electronic set-up for pulse width (~ 1 ns) measurements as represented in Fig. 1.1.19, one observes on a scope, by tuning the parameters of the accelerator pulsing system, the time performance, width and symmetry of the pulses. This system will be of interest in the future when attempts will be made to reduce the pulse width down to about 0.2 ns with a rebuncher.

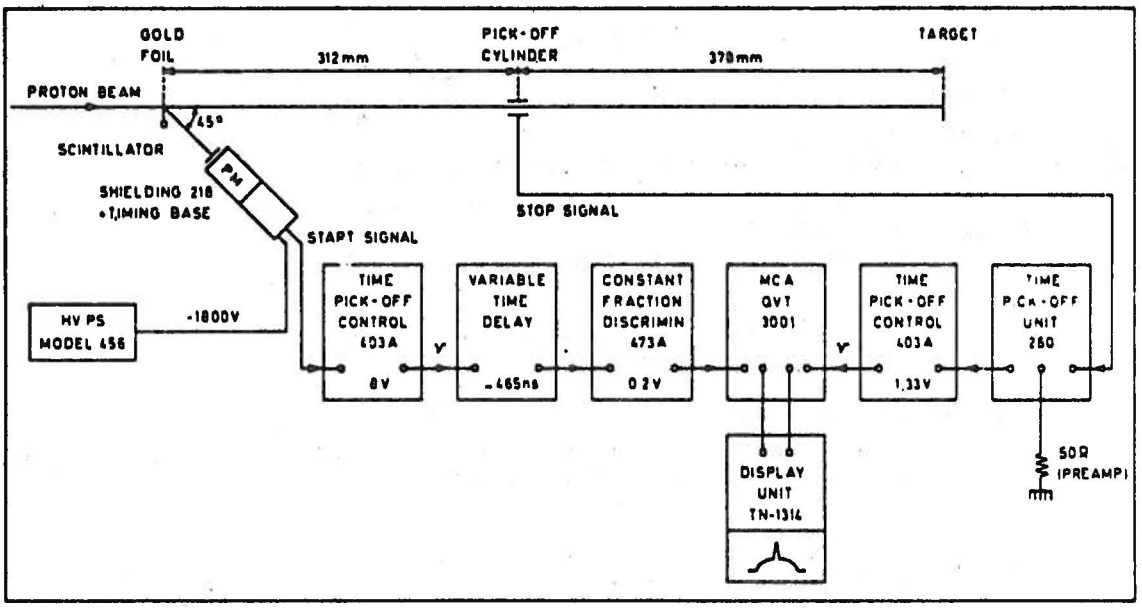

Figure 1119 Electronic set-up to measure the pulse width.

Theoretical studies on spiral and helix resonators used as rebuncher have been made (CBNM/VG/33/79).
A study on kinematics of neutron producing reactions has been published [17] with the following abstract:
Some aspects of the kinematics of neutron producing nuclear reactions are discussed. It is shown that the four parameters (Q, 3 masses) may be further reduced to three. In addition the usual neutron energy equation as a function of emission angle and incident ion energy is inverted to an equation giving the incident ion beam energy as a function of neutron energy and emission angle.

The value of the minimum neutron energy at backward emission angles for positive Q-value reactions is deduced as well as the value of the angle dependent forward threshold for negative Q-value reactions.
For selected input parameters such as nuclear reaction, energy and emission angle of neutrons, material and thickness of target, a programme, written in BASIC, gives as output the ion beam energy and for a given calibration constant, the corresponding nuclear magnetic resonance frequency.

REFERENCES

(1) R.B. PEREZ, G. de SAUSSURES, R.L. MACKLIN, J. HALPERIX, Phys. Rev. C20, 528 (1979).

(2) F. CORVI, G. ROHR, H. WEIGMANN, in Nuclear Cross Sections and Technology, NBS Spec. Pub. 425, (1975), Vol. II, p. 733.

(3) Proceedings of the Conference on Nuclear Cross Sections and Technology, Knoxville, October 22-26, 1979.

(4) J.B. CZIRR, G.W. CARLSON, Nucl. Sc. Engng. 64 (4) 1977, 892.

(5) R. GWIN, 1979, private communication by W. Benitz.

(6) F.H. FRÖHNER, report K.F.K. 2129, 1976.

(7) J. de SAUSSURES, D.K. OLSEN, R.B. PEREZ, report ORNL-TM-6286, 1978.

(8) F.G. PEREY et al., Neutron Data of Structural Materials for Fast Reactors, Geel, 1977, ed. by K.H. Böckhoff, Pergamon Press, p. 547.

(9) M.C. MOXON, private communication.

(10) A. PAULSEN, R. WIDERA, F. ARNOTTE, H. LISKIEN, "Cross Sections for the Reactions $^{54}Fe(n,\alpha)^{51}Cr$, $^{54}Fe(n,p)^{54}Mn$ and $^{56}Fe(n,p)^{56}Mn$" to be published as technical Note in Nucl. Sc. Eng.

(11) B. GOEL, Nucl. Sci. Eng. 69 (1979) 99.

(12) U. SEEBECK, M. BORMANN, Nucl. Phys. 68 (1965) 387.

(13) N.A. KHAN, S. MUBARAKMAND, MAHMUD AHMAD, Nucl. Phys. A202 (1973).

(14) G.P. DOLYA, A.P. KLYUCHAREV, V.P. BOZHKO, V. YA. GOLOVNYA, A.S. KACHAN, A.I. TUTUBALIN,
Proc. 3rd All-Union Conference on Neutron Physics, Kiev June 9-13, 1975, Part 4, p. 173.

(15) S.M. GRIMES, R.C. HAIGHT, K.R. ALVAR, H.H. BARSCHALL, R.R. BORCHERS,
Phys. Rev. C19 (1979) 2127.

(16) H. FARRAR IV, D.W. KNEFF,
Trans. Am. Nucl. Soc. 28 (1978) 197.

(17) A. CRAMETZ,
EUR 6313 EN. Eur. App. Res. Rep. Vol. 1 (2) 1979, p. 377.

1.2 NON NEUTRON NUCLEAR DATA

1.2.1 *Studies on the decay of $^{93}Nb^m$*

D. Reher, W. Oldenhof, R. Vaninbroukx

The measurements for the determination of the half-life of $^{93}Nb^m$ have been continued using Si(Li) detectors. Four sources prepared from two different samples have been measured 17 times over a period of 2.5 years.

The mean value of the preliminary result is: $T_{1/2}$ = (15.7 ± 1.0)y. This value, which is 2.6 % higher than the result obtained earlier, was compared with the value of (16.4 ± 0.4)y, published by R. Lloret [1]. Looking for possible systematic differences between both results, sources have been exchanged between CBNM and CEN Grenoble. Measurements started four mounths ago. But this is too short a time to reach a significant conclusion.

Measurements of conversion electrons have been restarted. Sources were prepared by sputtering technique bombarding niobium metal with Ar ions and collecting the ejected Nb on thin carbon foils. This procedure gave very thin sources which resulted in an improved electron energy resolution. The L-and M,N+... conversion electron peaks measured in vacuum with an open Si(Li) detector can clearly be distinguished as shown in Fig. 1.2.1.

In order to check whether $^{93}Nb^m$ could be produced by a (γ,γ') reaction, measurements have been performed on two niobium foils irradiated with a high gamma-ray dose (0.7-1 MeV, 10^{11} to 10^{13} rad) at SCK/CEN Mol. No Nb K X-rays could be found from the irradiated foils.

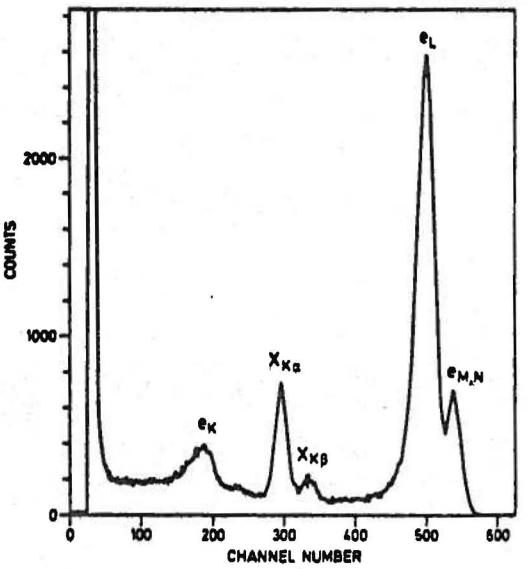

Figure 1.2.1 Conversion electron spectrum from a very thin $^{93}Nb^m$ source prepared by sputtering technique on a carbon foil. The measurement was performed under vacuum with an open Si(Li) detector.

A paper on the utilization of liquid scintillation counting techniques for decay parameter studies of radionuclides decaying via low energy isomeric transitions has been presented at the International Conference on Liquid Scintillation Counting, San Francisco [2]. The determination of various decay parameters of $^{93}Nb^m$ and $^{103}Rh^m$ has been described and a set of consistent values reported (see Table 1.2.1.).

Theoretical internal conversion coefficients for niobium (Z = 41), multipole order M4 and transition energy E_γ have been deduced from the tables of F. Rösel et al. [3] and from those of R.S. Hager and E.C. Seltzer [4]. A spline interpolation programme in FORTRAN IV was written for this purpose. The comparison, shown in Table 1.2.2., reveals that for the K and L shells differences are of the order of ± 3 %, but that for the higher M and N shells they become up to 8 %.

TABLE 1.2.1.

Experimental data of $^{93}Nb^{m}$ and $^{103}Rh^{m}$

Parameter	$^{93}Nb^{m}$	$^{103}Rh^{m}$
I_{KX}	0.116 ± 0.004	0.084 ± 0.005
I_{γ}	$(4.5 \pm 1.0).10^{-6}$	$(7.0 \pm 0.4).10^{-4}$
I_{eK}	0.155 ± 0.012	0.104 ± 0.009
α	$(2.2 \pm 0.4).10^{5}$	1430 ± 80
α_K	$(3.4 \pm 0.8).10^{4}$	148 ± 18
$T_{1/2}$	(15.7 ± 1.0)y	(56.1 ± 0.1)min

1.2.2 *Studies on the decay of ^{141}Ce*

H.H. Hansen

On the basis of the internal conversion data obtained during the decay data study of ^{141}Ce [5] calculations of the nuclear penetration effect upon the internal conversion process of the 1-forbidden M1-transition of 145.4 keV following the ^{141}Ce decay have been performed. Values of the nuclear penetration parameter λ and the E2/M1 multipole mixing ratio δ^2 have been deduced. The results have been published [6] together with those obtained for similar transitions in the decay of ^{139}Ce and ^{203}Hg (Table 1.2.3).

TABLE 1.2.3.

Nuclear Penetration Parameter λ and E2/M1 multipole mixing ratio δ^2 for 1-forbidden γ-ray transitions in ^{139}La, ^{141}Pr and ^{203}Tl

Nuclide	E_{γ} (keV)	λ	δ^2
^{139}La	165.8	2.8 ± 1.3	$(8.4 \,^{+\,14.0}_{-\,8.4}) \cdot 10^{-4}$
^{141}Pr	145.4	1.2 ± 0.6	$(4.8 \pm 0.5) \cdot 10^{-3}$
^{203}Tl	279.2	6.4 ± 1.1	1.36 ± 0.12

TABLE 1.2.2.

Comparison of theoretical internal conversion coefficients for niobium, M4, and E_γ = 30.75 keV

SHELL	α(RÖSEL)	α(HAGER, SELTZER)	$\frac{\alpha(\text{RÖ}) - \alpha(\text{HASE})}{\alpha(\text{RÖ})}$
K	$2.63\ 10^4$	$2.71\ 10^4$	- 0.030
L_1	$2.59\ 10^4$	$2.56\ 10^4$	0.012
L_2	$4.96\ 10^3$	$4.92\ 10^3$	0.008
L_3	$9.18\ 10^4$	$8.87\ 10^4$	0.034
L	$1.23\ 10^5$	$1.19\ 10^5$	0.033
M_1	$5.66\ 10^3$	$5.40\ 10^3$	0.046
M_2	$1.02\ 10^3$	$9.87\ 10^2$	0.032
M_3	$1.93\ 10^4$	$1.83\ 10^4$	0.052
M_4	$2.54\ 10^2$	$2.35\ 10^2$	0.075
M_5	$7.47\ 10^2$	$6.81\ 10^2$	0.088
M	$2.70\ 10^4$	$2.56\ 10^4$	0.052
N_1	$9.78\ 10^2$		
N_2	$1.48\ 10^2$		
N_3	$2.81\ 10^3$		
N_4	$1.85\ 10^1$		
N	$3.95\ 10^3$	$4.5\ 10^3$ a)	- 0.118
O_1	$7.60\ 10^1$		
TOTAL	$1.80\ 10^5$	$1.76\ 10^5$	0.022

a) This value is deduced from the tables of DRAGOUN et al. [13] by extrapolation to E_γ = 30.75 keV.

1.2.3 *Studies on the Decay of ^{133}Ba*

H.H. Hansen, D. Mouchel

The experiments for the half-life determination have been pursued. Two new sets of the ^{133}Ba photon spectrum have been measured with the Ge(Li) detector. Two different sources have been used. Up to now the decay has been followed for about 21 months. From 16 individual results a preliminary mean value for the half-life of (10.62±0.76)y can be given. The measurements with the NaI(Tl) γ-ray spectrometer have also been continued using three sources under five different geometrical conditions. In this experiment the ^{133}Ba decay has been followed during the last 5 years. A preliminary half-life value of (10.56 ± 0.15)y has been obtained. In both cases the stated uncertainties are standard deviations. Although in both types of experiments they are rather high the deduced half-life values agree within ± 0.3 %.

In 1978 a series of comparative measurements had shown that for electron energies > 200 keV a Si(Li) detector cooled by liquid nitrogen is very suitable for the electron detection in the magnetic β-spectrometer. Thus, for the current experiments a Si(Li) probe of 80 mm^2 sensitive area and 2 mm thickness has been used. First electron spectra have been recorded by scanning with small but equal current increments. The sources used for this study were prepared by drop deposition onto gold coated VYNS foils, so they were not especially suited for electron measurements at energies below 100 keV. Fig. 1.2.2 shows an example of the electron spectrum originating from the K-, L- and M-shell internal conversion of the transitions of 276.4, 302.9, 356.0 and 383.9 keV. This corresponds to electron energies between 240.4 keC (K-shell conversion electrons from the 276.4 keV transition) and 383.0 keV (M-shell conversion electrons from the 383.9 keV transition). The momentum resolution of 0.8 % for the most intense line in the spectrum shown (K-shell conversion electrons from the 356.0 keV transition) is due to the experimental conditions (baffles on slits) at which the magnetic β-spectrometer was operated. Measurements were made at several different instrumental resolution conditions.

The data are still under evaluation. The treatment of the spectra is rather complicated due to the overlapping of conversion electron lines of different shells and from various transitions. On the other hand, for the 160.6 keV transition the conversion electron lines of the K and L+M+... shells appear well separated in the spectra. In this case the data treatment was straightforward and resulted in a preliminary value for the conversion ratio of K/(L+M+...) = 3.6 with a standard deviation of ± 6 % relative.

On the other hand it has turned out that for the registration of conversion electron spectra at energies below 100 keV the liquid-nitrogen-cooled Si(Li) detector is not well suited. This is due mainly to an unfavourable signal/noise ratio and to oscillations from outside, e.g. via the mains voltage, disturbing the pulse treatment system. Therefore, another detection system has been designed. It consists of a plastic scintillator with a high light yield, a photomultiplier with low noise characteristics and a power supply uncoupled from the mains supply.

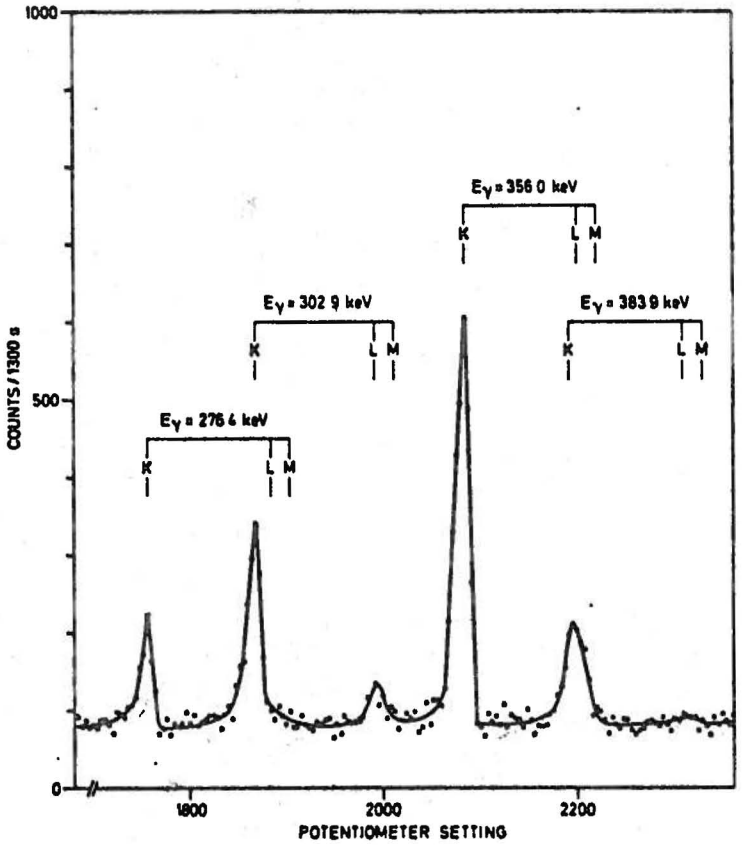

Figure 1.2.2 Partial internal conversion electron spectrum as scanned with the magnetic β-spectrometer. Groups of K-, L- and M-shell conversion electrons are indicated with the corresponding γ-ray energies.

1.2.4 *Studies of the decay of* ^{241}Pu

P. De Bièvre, M. Gallet

The determination of the half-life of ^{241}Pu by direct decay measurements using mass spectrometric methods have been continued. Samples of a Pu material containing 92.7 % ^{241}Pu at the beginning of the measurements have been measured over a period of about 3 years. During that period about 14 % of the ^{241}Pu atoms present at the beginning have decayed. The preliminary result of the measurements performed up to now is: $T_{1/2}$ = 14.45 years, with an estimated uncertainty of about ± 1 %.

1.2.5 *Studies on the decay of* ^{238}Pu

R. Vaninbroukx, G. Grosse

The intensities of the photons emitted in the energy range 10-50 keV in the decay of ^{238}Pu have been determined experimentally. Two calibrated Si(Li) detectors were used. The detectors were calibrated using reference samples of suitable radionuclides. The photon intensities for the peak-efficiency calibration were obtained from a survey of

literature data and from our own experimental work. The accuracy of the calibration curves is estimated to be 2-3 % corresponding to a 1σ confidence level. Four ^{238}Pu sources, prepared from an isotopically pure ^{238}Pu sample, were measured with both detectors. A typical photon spectrum is shown in Fig. 1.2.3.

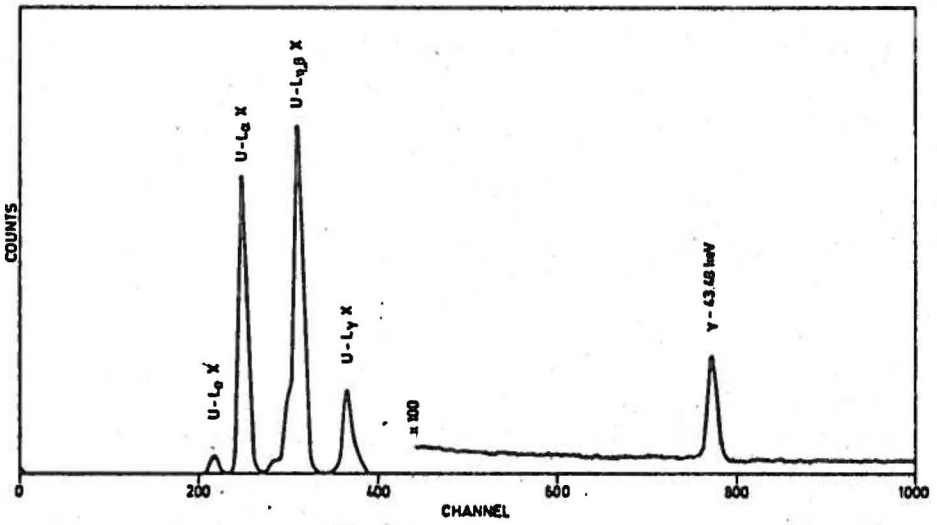

Figure 1.2.3 Photon spectrum of ^{238}Pu.

The results of these measurements are summarized in Table 1.2.4. The quoted uncertainties, corresponding to a 1σ confidence level, take into account systematic and random effects.

TABLE 1.2.4.

Photon intensities in the decay of ^{238}Pu

Radiation	Mean energy (keV)	Intensity (photon/decay)
U-L_ℓ X	11.6	0.0026 ± 0.0001
U-L_α X	13.6	0.0408 ± 0.0012
U-$L_{\eta,\beta}$ X	17.2	0.0570 ± 0.0017
U-L_γ X	20.2	0.0137 ± 0.0004
Total LX		0.1141 ± 0.0034
γ-43	43.48	(3.93 ± 0.12) 10^{-4}

The values obtained for the LX-ray intensities are about 25 % lower than those measured by VASILIK and MARTIN [7] but they agree within less than 2 % with those of BEMIS and

TUBBS [8]. Our value of 0.114 ± 0.003 for the total LX-ray intensity is exactly the same as that obtained by SWINTH [9] using a solid state (X-ray)-(α-particle) coincidence counter. The intensity obtained for the 43.5 keV γ ray is in close agreement with the result of GUNNINK et al. [10].

As a by-product of these measurements one can deduce the total internal conversion coefficient for the 43.5 keV transition. The result of 730 ± 40 is about 8 % lower than the experimental results of DUKE and TALBERT [11] and of SCHLENKER [12] but is in reasonable agreement with the theoretical value of 715 ± 20 obtained by interpolation of the tabulated values of HAGER and SELTZER [4] and applying a correction for the N+ ... contribution from the experimental (N+ ...)/(L+M) ratio of AMTEY et al. [14].

1.2.6 *Determination of half-lives of ^{57}Co and ^{109}Cd*

R. Vaninbroukx, G. Grosse

Several sources of ^{57}Co and ^{109}Cd were used for checking the long-term stability of the detection efficiency of Si(Li) detectors in the energy range between 10 keV and 25 keV for the half-life measurements on $^{93}Nb^{m}$. As a check of the sources they were remeasured at regular intervals over the whole period of observation with a 7.5 cm x 7.5 cm NaI(Tl) detector for which the long-term reproducibility is known to be better than ± 0.05 %. These measurements were used for the calculation of the half-lives of these radionuclides. The results obtained till now are summarized in Table 1.2.5. where the uncertainties quoted are at the 1σ level taking into account random and systematic effects.

TABLE 1.2.5.

Preliminary results of the half-lives of ^{57}Co and ^{109}Cd

Nuclide	Number of sources	Number of solutions of different origins	Period of observation in half-lives	Half-life in days
^{57}Co	8	4	3.0	271.9 ± 0.2
^{109}Cd	6	3	2.0	461.7 ± 0.4

1.2.7 *Decay of ^{224}Ra*

D. Reher

In the frame of a project of dating groundwaters by measurement of uranium and thorium isotope disequilibria, the relative α emission probability of the 5.45 MeV α transition to the excited level of 241 keV in the ^{224}Ra decay is of relevance. The emission probability of about 5.5 % is only known with a relative accuracy of 10 %. The

5.45 MeV α line is located under the 5.42 MeV main peak of ^{228}Th, the spike used by most of the laboratories of the Uranium Series Intercomparison Project (USIP). The nuclide ^{224}Ra belongs to the ^{232}U decay chain. If the ^{232}U is separated, ^{224}Ra and the subsequent daughters will be in equilibrium with the parent nuclide ^{228}Th after a relatively short time. First experiments have been made with a ^{228}Th source encapsulated in an Al container. The source material is at least 13 years old. The emission rate of the 241 keV γ-ray line from the ^{224}Ra decay was determined relative to the emission rate of the 238.6 keV γ-ray line from the ^{212}Bi decay, the value of which was taken from the latest ENSDF version. Several corrections had to be applied such as the internal conversion in the 241 keV γ-ray transition, the different efficiencies for the 241 keV and the 238.6 keV γ lines in the detector and the different absorption of these γ rays in the Al source container.
The high purity germanium detector of a Low Energy X-ray and Electron Spectrometer was used to measure the γ-ray spectrum around 240 keV of a ^{228}Th source. At this energy the resolution of the detector is 1.1 keV and its efficiency for this energy is of the order of 15 %. The problem is to separate both peaks from each other and to determine their respective intensities. This was done with the programme RETEOH which is a version of the programme CUTIPIE [15].
A preliminary value of 0.054 ± 0.002 was found. This result will become more accurate by improving the spectrum resolution, determining the relative emission probability of the 238.6 keV γ-ray line from the ^{212}Bi decay and by improving the evaluation of the spectra.

1.2.8 *Half-life of excited nuclear levels*

A. Nylandsted-Larsen, H.H. Hansen, D. Mouchel

The determination of the half-life of the first excited nuclear level of ^{119}Sn at 23.87 keV by the delayed coincidence technique has been finished. Two different types of sources have been used in these experiments with various detector combinations. A very pure source was made by implanting ^{119}Sn^{m} in a plastic scintillator by an isotope separator. This source could be used simultaneously as source and as detector. The other source was made by drying a drop of a solution. The mean value of 21 measurements is $T_{1/2}$ = (18.03 ± 0.07)ns. The uncertainty quoted corresponds to the 1σ level and takes into account both random (0.2 %) and systematic (0.2 %) effects. A paper describing the experiment, its results and their statistical evaluation has been published [16].
The final evaluation of the half-life of the first excited nuclear level of ^{133}Cs at 81.0 keV was completed. The mean value of 10 measurements is $T_{1/2}$ = (6.22 ± 0.03)ns. The quoted uncertainty takes into account both statistical (0.3 %) and systematic (0.2 %) uncertainties (1σ confidence level).

1.2.9 *International comparison of activity measurements of a ^{134}Cs solution*

A. Nylandsted-Larsen, E. Celen, W. Oldenhof, W. Zehner

At the beginning of October 1978 CBNM received two ampoules of 5 ml CsCl in 0.2 N HCl with a carrier content of 20 μg of CsCl per g of solution. The activity concentration was about 800 kBq g^{-1}. Fourteen sources were prepared by drop evaporation and by freeze drying. The source activity has been determined by the 4 $\pi\beta$-γ coincidence counting extrapolation method varying the detection efficiency in the β channel by covering the source with gold coated VYNS foils. The total uncertainty on the activity concentration of the ^{134}Cs solution corresponding to a 1σ confidence level was found to be 0.09 %, composed of 0.04 % random and 0.05 % systematic uncertainty. The result was communicated to BIPM in January 1979.
In total 24 laboratories participated in this intercomparison. The standard deviation of the results of the participants, disregarding two outliers, was reported to be 0.15%.

1.2.10 *International comparison of activity measurements of a ^{137}Cs solution*

A. Nylandsted-Larsen, E. Celen, G. Grosse, R. Vaninbroukx, W. Zehner

Parallel to the large scale comparison of activity measurements of a ^{134}Cs solution a small scale comparison of activity measurements of a ^{137}Cs solution took place. This comparison was finished 1st March 1979. Participants were AECL, CBNM, NBS, NPL, NRC, OMH and PTB. The objective was to determine the activity concentration of the solution by the efficiency tracing technique using the standardized ^{134}Cs solution from the large scale comparison as tracer. Nine quantitative sources were measured with this technique and three sources were measured with an efficiency calibrated NaI(Tl) detector. The results from these two methods agreed to within 0.02 %. The total uncertainty on the activity concentration determined by the efficiency tracer technique was found to be 0.27 % on a 1σ confidence level, being composed of 0.13 % random uncertainty and 0.14 % systematic uncertainty.

1.2.11 *International comparison of activity measurements of a ^{55}Fe solution*

R. Vaninbroukx, W. Bambynek, G. Grosse, A. Kacperek, W. Oldenhof, D. Reher, W. Zehner

At the last meeting of Section II (Measurement of Radionuclides) of the BIPM Consultative Committee on Measuring Standard for Ionizing Radiation in June 1977 [17] it was decided to organize an international comparison of activity measurements of a ^{55}Fe solution. This is the first intercomparison of a pure electron capture nuclide. The solution was distributed by NPL, Teddington, on behalf of BIPM. Measurements started at CBNM in February using the following methods: (a) liquid scintillation counting; (b) counting of X-ray and Auger electrons in a 4π proportional counter operated under high pressure; (c) efficiency tracing techniques using ^{51}Cr and ^{54}Mn as tracers; (d) counting of K X-rays with a calibrated Si(Li) detector; (e) calibration relative to a standardized ^{54}Mn source using a Si(Li) detector.

The Auger electron measurements (b) were not successful because of the high degree of self-absorption in the source material. The 4π proportional counter operated under high pressure could only be used for the K X-ray measurements. The efficiency tracing technique (c) using ^{51}Cr and ^{54}Mn as tracers was also insufficient. It was not possible to prepare stable sources on Au-coated VYNS foils, neither from the hydrochloric acid tracer solutions nor from the nitric acid ^{55}Fe solution. The results obtained with the other methods have been communicated to BIPM, together with a short description of the methods and the nuclear constants used. The results are summarized in Table 1.2.6. The quoted uncertainties correspond to a 1σ confidence level. The project is finished.

TABLE 1.2.6.

Preliminary results of the ^{55}Fe calibration

Method	Radioactivity concentration at the reference date (Bq mg^{-1})	Uncertainties (%)	
		Random	Systematic
Liquid scintillation	4040	1.0	1.4
4π proportional pressure	4040	0.5	2.6
Calibrated Si(Li)	3970	0.2	2.6
Relative to ^{54}Mn	3980	0.2	0.8

1.2.12 *International comparison of the ^{133}Ba photon emission rates*

H.H. Hansen, R. Vaninbroukx

The ICRM initiated an international comparison of photon emission rate measurements for low energy photons in the energy range 30 to 400 keV. ^{133}Ba was chosen as multi-photon-emitting radionuclide. Participants of the study are mainly members of the ICRM and ICRM Working Groups. It was asked to determine the emission rates of the K_α and K_β X rays and the 9 γ rays occuring in the decay. The experiments were performed with sources of known amount of radioactive material prepared from a $BaCl_2$ solution. Four sources encapsulated in small Al-containers were used for the Ge(Li) measurements (γ rays with $E_\gamma \geq 160$ keV) and six sources prepared on chromium coated glass plates were used for the Si(Li) measurements (X rays and γ rays below 100 keV).
Table 1.2.7. shows the photon emission probabilities per decay for the different photons. The quoted uncertainties correspond to a 1σ confidence level and represent a combination of statistical and estimated systematic uncertainties.

TABLE 1.2.7.

Results of the photon emission probabilities as determined in the frame of the ICRM international comparison on ^{133}Ba X and γ rays

Photon	Energy (keV)	Emission probability per decay
$X_{K\alpha}$	30.8	1.007 ± 0.013
$X_{K\beta}$	35.2	0.232 ± 0.003
γ_1	53.1	0.0219 ± 0.0003
$\gamma_2 + \gamma_3$	80.9 *	0.360 ± 0.006
γ_4	160.6	0.0066 ± 0.0001
γ_5	223.2	0.0045 ± 0.0001
γ_6	276.4	0.0721 ± 0.0005
γ_7	302.9	0.1845 ± 0.0014
γ_8	356.0	0.621 ± 0.004
γ_9	383.9	0.0902 ± 0.0006

* E_{γ_2} = 79.6 keV, E_{γ_3} = 81.0 keV.

1.2.13 *Niobium dosimetry intercomparison*

D. Reher, R. Vaninbroukx

The objective of this interlaboratory dosimetry comparison is to compare measuring techniques, to improve the calibration of the various equipments, and to define the parameters used for the interpretation of niobium measurements. Furthermore, it is expected to improve the knowledge of the $^{93}Nb(n,n')$ cross-section and to learn more about the influence of impurities in niobium. Foils with very low tantalum content were supplied by the Max-Planck-Institut für Metallforschung, Stuttgart. They were irradiated in the fast breeder reactor EBR II, at Hanford, but could not be recovered entirely because they were damaged during the irradiation. Therefore some foils from an irradiation in BR2 Mol were also measured and evaluated. CBNM received five pieces of different materials and irradiations. Impurity measurements have been completed and preparations for the calibration have been finished. The measurements have been started and the results will be communicated to SCK/CEN Mol, the organizing laboratory in the beginning of 1980.

1.2.14 *Interlaboratory alpha-spectrum evaluation programme AS-76*

G. Bortels, J. Broothaerts, P. De Bièvre, M. Gallet, W. Wolters,
I.L. Barnes *, K.M. Glover **

The AS-76 intercomparison was organised as a joint safeguards project of the Kernforschungszentrum Karlsruhe, and CBNM, Geel. The objective was to determine the present spread in the α-spectrometric measurement of the activity ratio $^{238}Pu/(^{239}Pu + ^{240}Pu)$ under routine conditions. Four sample solutions have been used. Three of them were prepared from input solutions of a reprocessing plant containing about 0.2 %, 0.8 % and 1.6 % of ^{238}Pu. A fourth solution with about 0.9 % ^{238}Pu originated from a reprocessed Pu solution.

The sample solutions have been characterized by α spectrometry at CBNM, Geel and AERE, Harwell, to certify the activity ratio mentioned above, and by mass spectrometry at NBS, Washington and at CBNM, Geel, to certify the isotopic composition. The characterization work was coordinated by CBNM.

The results are given in Tables 1.2.8.and 1.2.9.

TABLE 1.2.8.

Results of the AS-76 Sample Characterization by α-Particle Spectrometry

Nominal ^{238}Pu abundance (%)	α-Activity Ratios $^{238}Pu/(^{239}Pu + ^{240}Pu)$		
	C B N M	A E R E	M e a n
0.8	1.4463 ± 0.0043(0.30%)	1.4455 ± 0.0043(0.30%)	1.446 ± 0.004(0.30%)
1.6	2.984 ± 0.010 (0.35%)	2.9866 ± 0.009 (0.30%)	2.985 ± 0.010(0.35%)
0.9	1.6361 ± 0.0057(0.35%)	1.6382 ± 0.0050(0.30%)	1.637 ± 0.006(0.35%)

The indicated accuracies corresponds to a 3σ confidence level and include an estimate of the systematic uncertainties. For the calculation of the atom ratios from the measured activity ratios, as given in Table 1.2.8., the following half-lives have been used [18] $T_{1/2}(^{238}Pu)$ = 87.74 ± 0.09 years, $T_{1/2}(^{239}Pu)$ = 24100 ± 30 years and $T_{1/2}(^{240}Pu)$ = 6553 ± 8 years. The samples containing about 0.2 % of ^{238}Pu were found to be inhomogeneous. This solution had been prepared by spiking a given input solution successively with enriched ^{239}Pu and ^{240}Pu. Differences in the α-activity ratio up to about 3 % have been observed and a linear relationship was observed between the atom

---

* National Bureau of Standards, Washington, U.S.A.

** Atomic Energy Research Establishment, Harwell, U.K.

TABLE 1.2.9.

Values and Accuracies of the Atom Ratios of $^{238}Pu/^{239}Pu$ in Samples from Different Characterization Laboratories and Methods

Nominal ^{238}Pu abundance (%)	Values and Accuracies of the Atom Ratios $^{238}Pu/^{239}Pu$			
	From α-Spectrometric Measurements of Activity Ratios $^{238}Pu/(^{239}Pu + ^{240}Pu)$		From Mass Spectrometric Measurements	
	C B N M	A E R E	N B S	C B N M
0.8	0.01224 ± 1.0 %	0.01223 ± 1.0 %	0.01212 ± 1.2 %	0.01221 ± 0.7 %
1.6	0.02596 ± 1.0 %	0.02598 ± 1.0 %	0.02598 ± 0.57%	0.02596 ± 0.7 %
0.9	0.01440 ± 1.0 %	0.01442 ± 1.0 %	0.01425 ± 1.1 %	0.01436 ± 0.7 %

ratio of $^{239}Pu/^{240}Pu$ from mass spectrometry and the α-activity ratio of $^{238}Pu/(^{239}Pu + ^{240}Pu)$. It is assumed that the inhomogeneity is due to particulate matter present in the solution. The results have been presented to the First Symposium on Safeguards and Nuclear Material Management, 25 and 26 April 1979 at Brussels [19].

1.2.15 *Compilations and Evaluations*

Internal conversion data

H.H. Hansen

The internal conversion data compilation has been completed. The proofreading of a listing of about 800 references has been accomplished. For the evaluation of the internal conversion coefficients and ratios 17 transitions in 14 nuclides (e.g. ^{7}Be, ^{57}Co, ^{137}Cs, ^{139}Ce, ^{141}Ce, ^{198}Hg, ^{203}Hg, ^{241}Am) have been selected. The energies are between 60 and 1333 keV. Most of the nuclides have simple decay schemes and may be well suited for photon and electron detector calibration work.

Fluorescence yields

W. Bambynek

The reevaluation of X-ray fluorescence yields was continued in order to incorporate new results into the list of recommended data which was published seven years ago. The main effort has been spent on evaluating K-shell data. About 50 new experimental values have been compiled and partly evaluated.

Decay data of actinides
R. Vaninbroukx

The status file on the half-life of ^{239}Pu was updated. A value of (24.114 ± 25)y is recommended. The quoted uncertainty, corresponding to a 1σ confidence level, takes into account statistical and systematic effects.
A review paper on nuclear decay data and α-induced neutron generation relevant to Pu-contaminated waste was presented at the International Meeting on Monitoring of Pu-Contaminated Waste [20]. This paper was also discussed at a IAEA meeting (Cadarache in May 1979), in which the decay data, including spontaneous fission half-lives, of all actinides were critically reviewed. Possibly, the available nuclear decay data are sufficiently accurate for waste control.

Critical survey of data sources
W. Bambynek

A survey of the most important compilations and evaluations in the nuclear field is in preparation. CBNM is responsible for the data sources on nuclear decay and radioactivity. About 70 relevant papers have been compiled. The critical review of these papers is in progress.

REFERENCES

(1) R. LLORET,
Mesure de la période de décroissance radioactive de $^{93}Nb^{m}$,
Radiochem. Radioanal. Letters 29, 165 (1977).

(2) R. VANINBROUKX,
The use of liquid scintillation counting techniques for decay parameters studies of redionuclides decaying via low energy isomeric transitions.
International Conference on Liquid Scintillation Counting, August 21-24, 1979, San Francisco, in press.

(3) F. RÖSEL, H.M. FRIES, H.C. PAULI,
Internal conversion coefficients for all atomic shells,
Atomic Data and Nucl. Data Tables 21, 91 (1978).

(4) R.S. HAGER, E.C. SELTZER,
Internal conversion tables,
Nucl. Data Tables A4, 1 (1968).

(5) H.H. HANSEN, E. CELEN, G. GROSSE, D. MOUCHEL, A. NYLANDSTED-LARSEN, R. VANINBROUKX,
The decay of ^{141}Ce.
Z. Physik, A290, 113 (1979).

(6) H.H. HANSEN,
Nuclear Structure effect on internal conversion of 1-forbidden transition in ^{139}La, ^{141}Pr, and ^{203}Tl.
Z. Physik, A291, 43 (1979).

(7) R.G. VASILIK, R.W. MARTIN,
$UL_{\alpha,\beta\gamma}$ X-ray intensities from the alpha decay of ^{238}Pu,
Nucl. Instr. Methods 135, 405 (1976).

(8) C.E. BEMIS Jr., L. TUBBS,
Absolute L-series X-ray and low-energy gamma-ray yields for most transuranium nuclides, in: O.L. KELLER (ed.) Chemistry Division Annual Progress Report for Period Ending March 31, 1977, Oak Ridge National Laboratory Report, ONRL-5297 (1977), p. 92.

(9) K.L. SWINTH,
A solid state X-ray-alpha coincidence counter,
IEEE Trans. Nucl. Sci. NS-18, 125 (1971).

(10) R. GUNNINK, J.E. EVANS, A.L. PINDLE,
A reevaluation of the gamma-ray energies and absolute branching intensities of ^{237}U, $^{235,239,240,241}Pu$, and ^{241}Am.
Lawrence Livermore Laboratory Report,
UCRL-52139 (1978).

(11) C.L. DUKE, W.L. TALBERT Jr.,
Total internal conversion coefficients for low-energy E2 transitions in ^{224}Ra, ^{228}Th, ^{234}U, ^{236}U, and ^{240}Pu.
Phys. Rev. 173, 1125 (1968).

(12) R.A. SCHLENKER,
in : R.D. EVANS, R.J. KOLENKOW (eds.)
Radium and Mesothorium Poisoning and Dosimetry and Instrumentation Techniques in Applied Radioactivity,
Annual Progress Report MIT-952-5, Part I, p. 200 (1968).

(13) O. DRAGOUN, Z. PLAJNER, F. SCHMUTZLER,
Contribution of outer atomic shells to total internal conversion coefficients.
Nucl. Data Tables A9, 119 (1971).

(14) S.R. AMTEY, J.H. HAMILTON, A.V. RAMAYYA, M.M. MLADJENOVIC,
L and M subshell ratios of the 43.5 keV E2 transition in ^{234}U,
Nucl. Phys. A 126, 201 (1969).

(15) W. TEOH,
CUTIPIE, a computer programme to analyse gamma-ray spectra,
Nucl. Instr. Methods 109, 509 (1973).

(16) A. NYLANDSTED-LARSEN, D. MOUCHEL, H.H. HANSEN,
Half-life of the 23.87 keV level in ^{119}Sn,
Z. Physik A294, 191 (1980).

(17) Comité Consultatif pour les Etalons de Mesure des Rayonnements Ionisants, Section II - Mesure des Radionucléides, 4ème Réunion, 14-16 juin, 1977 (Bureau International des Poids et Mesures, Pavillon de Breteuil, F-92310, Sèvres).

(18) A. LORENZ,
First coordinated Research Meeting on the Measurement of Transactinium Isotope Nuclear Data, Vienna, 20-21 April 1978,
INDC(NDS)-96/N (1978).

(19) G. BORTELS, P. DE BIEVRE, L. BARNES, K. GLOVER,
Characterization of the samples used in the AS-76 interlaboratory experiment.
1st Annual Symposium on Safeguards and Nuclear Material Management.
Brussels, B., April 25-27, 1979, ESARDA 10., STANCHI, L (Ed.)
(Publication Service of the JRC, Ispra, 1979), p. 380

(20) A. PAULSEN, R. VANINBROUKX,
Review on nuclear decay data and alpha-induced neutron generation relevant to Pu-contaminated waste.
International Meeting on Monitoring of Pu-Contaminated Waste, September 25-28, 1979. Ispra, in press.

ANNEX 1: LIST OF PUBLICATIONS, CONFERENCE PAPERS AND REPORTS

NUCLEAR MEASUREMENTS

Publications in periodicals

BASTIAN, Cl.
Discrimination of counting fluctuations in multichannel spectra.
Nucl. Instr. Methods, 159, 221 (1979).

CRAMETZ, A.
Kinematics of neutron producing reactions.
European Applied Research Reports, 1, 377 (1979), EUR 6313e (1979).

HANSEN, H.H., CELEN, E., GROSSE, G., MOUCHEL, D., NYLANDSTED-LARSEN, A., VANINBROUKX, R.
The decay of ^{141}Ce.
Z. Physik A., 290, 113 (1979).

HANSEN, H.H.
Nuclear structure effects on internal conversion of 1-forbidden transitions in ^{139}La, ^{141}Ar and ^{203}Tl.
Z. Physik A., 291, 43 (1979).

KNITTER, H.-H., BUDTZ-JØRGENSEN, C.
Measurements of the neutron fission cross-section of ^{241}Am from 100 eV to 5.3 MeV.
Atomkernenergie, 33, 205 (1979).

LISKIEN, H.
The particle spectrum to be expected from a d-t plasma.
Nucl. Sc. Eng., 71, 57 (1979).

MEWISSEN, L., POORTMANS, E., CORNELIS, E., VANPRAET, G., ANGELETTI, A., ROHR, G., WEIGMANN, H.
Neutron resonance parameters for Neptunium-237.
Nucl. Sc. Eng., 70, 155 (1979).

PAULSEN, A., WIDERA,R., ARNOTTE, F., LISKIEN, H.
Cross sections for the reactions ^{54}Fe(n,α)^{51}Cr, ^{54}Fe(n,p)^{54}Mn and ^{56}Fe(n,p)^{56}Mn.
Nucl. Sc. Eng., 72, 113 (1979).

VIESTI, G., LISKIEN, H.
The ^{10}B(n,$\alpha\gamma$)^{7}Li cross section between 0.1 and 2.2 MeV.
Ann. Nucl. Energy, 6, 13 (1979).

WEIGMANN, H., MANAKOS, P.
Deuteron exchange mechanism for the ^{6}Li(n,α) reaction at low energy.
Z. Physik A., 289, 383 (1979).

WEIGMANN, H., RAMAN, S., HARVEY, J.A., MACKLIN, R.L., SLAUGHTER, G.G.
Neutron resonances in ^{100}Mo and valence neutron capture.
Phys. Rev. C., 20, 115 (1979).

Contributions to conferences

BOCKHOFF, K.H. (Ed.)
Proceedings of a Specialists' Meeting on Neutron data of structural materials for fast reactors.
C.B.N.M. - Geel, B., 5-8 December 1977.
EUR 6108.
Pergamon Press - Oxford, U.K. 1979.

BRUSEGAN, A., CORVI, F., PASQUARIELLO, G., ROHR, G., SHELLEY, R., VAN DER VEEN, T., CORNELIS, E., MEWISSEN, L., POORTMANS, F.
Neutron transmission and capture measurements of separated Fe isotopes.
Ibidem. - p. 606.

PAULSEN, A.
Status report about some activation, hydrogen and helium producing cross-sections of structural materials.
Ibidem. - p. 261.

ROHR, G.
Evaluation and calculation of some average resonance parameters for structural materials.
Ibidem. - p. 614.

WEIGMANN, H., HARVEY, J.A., MACKLIN, R.L., RAMAN, S., SLAUGHTER, G.G.
Resonance parameters capture γ-rays and reaction mechanism in ^{98,100}Mo+n.
Ibidem. - p. 739.

BLONS, J., MAZUR, C., PAYA, D., RIBRAG, M., WEIGMANN, H.
Mesures à haute résolution et analyse de la section efficace de fission de ^{230}Th.
International Symposium on Physics and Chemistry of Fission.
I.A.E.A.-Vienna.
Jülich (D), 14-18 May 1979.
IAEA-SM 241, B.10 (1979).

BLONS, J., MAZUR, C., PAYA, D., RIBRAG, M., WEIGMANN, H.
Etats de vibration et rotation dans la réaction ^{233}Th(n,f).
Ibidem.
IAEA-SM 241, B.9 (1979).

KNITTER, H.-H., BUDTZ-JØRGENSEN, C., JENSEN, A.S.
Measurements of the neutron induced fission cross-section of Am-241 from 100 eV to 5.3 MeV.
Ibidem.
IAEA-SM 241, p.23 (1979).

BORTELS, G., DE BIEVRE, P., BARNES, L., GLOVER, K.
Characterization of the samples used in the AS-76 interlaboratory experiment.
1st Annual Symposium on Safeguards and Nuclear Material Management.
Brussels, B., April 25-27, 1979, ESARDA 10., STANCHI, L (Ed.)
(Publication Service of the JRC, Ispra, 1979), p. 380.

BUDTZ-JØRGENSEN, C., KNITTER, H.H.
Fast fission chambers to be used with highly active samples.
Fachausschuss Kernphysik Deutsche Physikalische Gesellschaft (D.P.G.),
26-30 März. 1979, Vorhandlungen DPG(VI), 14, 904 (1979).

KNITTER, H.-H.
Report on the November 1978 NEANDC-sponsored workshop on the cross-sections of the heavier Plutonium and Americium isotopes complemented by the status and accuracy of experimental neutron cross section data for elements higher than Americium.
Second Advisory Group Meeting on Transactinium Nuclear Data,
Cadarache (F), 30 April - 5 May 1979, to be published by IAEA Vienna.

LISKIEN, H., BUDTZ-JØRGENSEN, C., KNITTER, H.-H., PAULSEN, A.
Recent developments of special detection systems at the Van de Graaff laboratory of CBNM.
IX Symposium on Interaction of Fast Neutrons with Nuclei. T.U. Dresden (G.D.R.)
Sekt. Physik Gaussig (Dresden), 26-30 November 1979.

WAGEMANS, C., WEGENER-PENNING, G., WEIGMANN, H., BARTHELEMY, R.
Fission fragments mass- and energy- distributions for the neutron induced fission of ^{239}Pu in function of the resonance spins.
Physics and Chemistry of fission - IAEA. Jülich - F.R. Germany, May 1979.

VANINBROUKX, R.
Status report from CBNM-JRC to the second coordinated research meeting on the measurement of transactinium nuclear decay data.
A. LORENZ (ed.), Second coordinated research meeting on the measurement and evaluation of transactinium isotope nuclear data, Aix-en-Provence, F., 30 April - 1 May 1979.
INDC(NDS)-105/N (IAEA Nuclear Data Section, Vienna, 1979), p. 45.

VANINBROUKX, R.
Half-life of ^{239}Pu: present status.
A. LORENZ (ed.), Second coordinated research meeting on the measurement and evaluation of transactinium isotope nuclear data, Aix-en-Provence, F., 30 April - 1 May 1979.
INDC(NDS)-105/N (IAEA Nuclear Data Section, Vienna, 1979), p. 49.

Reports

BORTELS, G., BROOTHAERTS, J., DE BIEVRE, P., GALLET, M., WOLTERS, W.
Sample preparation for AS-76.
The AS-76 interlaboratory experiments on the alpha spectrometric determination of Pu-238.
Part III: Preparation and characterization of samples.
KfK.2862/EUR 6402e, p. 1 (1979).

BORTELS, G., BARNES, I.L., DE BIEVRE, P., GLOVER, K.M.
Characterization of the AS-76 samples.
Ibidem.
KfK.2862/EUR 6402e, p. 14 (1979).

BORTELS, G.
AS-76 characterization by alpha particles spectrometry at CBNM Geel.
Ibidem.
KfK.2862/EUR 6402e, p. 24 (1979).

SPANNAGEL, G., BEYRICH, W., BORTELS, G.
The AS-76 interlaboratory experiment on the alpha spectrometric determination of Pu-238.
Part II: Collection and evaluation of representative spectra.
KfK.2861/EUR 6401e (1979).

NUCLEAR MATERIALS

Publications in periodicals

BARFOOT, K.M., MITCHELL, I.V., ESCHBACH, H.L., MASON, P.I., GILBOY, W.B.
The analysis of air particulate deposits using 2 MeV protons.
J. Radioanal. Chem., 53, 255 (1979).

BERTHELOT, Ch., CARRARO, G., VERDINGH, V.
The use of photon activation analysis for the determination of Sm, Eu, Gd and Dy in boron carbide.
J. Radioanal. Chem., 50, 185 (1979).

MICHELENA, J.A., MÜSCHENBORN, G., VANSANT, E., DE BIEVRE, P.
Experimental evidence for oxygen isotope exchange between CO_2 molecules adsorbed in NaY zeolite at 0°C.
J.C.S. Chemical Communications, nr. 14, 619 (1979).

MITCHELL, I.V.
Rutherford backscattering applied to the analysis of materials and surfaces.
Phys. Bull., 30, 23 (1979).

MITCHELL, I.V., DOBMA, W.D.
Simple, robust and accurate model making of UHV systems.
J. Vac. Sc. Techn., 16, 88 (1979).

PAUWELS, J.
The contribution of nuclear analysis methods to the certification of BCR reference materials for non-metals in non-ferrous metals.
J. Radioanal. Chem., 50, 115 (1979).

Contributions to conferences

PAUWELS, J., TJOONK, J.
Spraypainting of deposits for nuclear measurements.
World Conference of the International Nuclear Target Development Society.
Technische Universität München,
München, D., 11-14 September 1978.
Nucl. Instr. Methods, 167, 77 (1979).

PAUWELS, J., VAN CRAEN, J., VAN GESTEL, J., VAN AUDENHOVE, J.
Polyimid substrate foils for nuclear targets.
Ibidem.
Nucl. Instr. Methods, 167, 109 (1079).

VAN AUDENHOVE, J., PEETERMANS, F., PAUWELS, J., VERBRUGGEN, A., DE BIEVRE, P., GALLET, M.
The preparation and characterization of reference fission foils.
Ibidem.
Nucl. Instr. Methods, 167, 61 (1979).

Reports

BORTELS, G., BROOTHAERTS, J., DE BIEVRE, P., GALLET, M., WOLTERS, W., GLOVER, K.M., KING, M., WILTSHIRE, R.A.P., GARNER, E.L., MACHLAN, L.E., BARNES, I.L.
The AS-76 interlaboratory experiment on the alpha spectrometric determination of Pu-238.
Part III: Preparation and characterization of samples.
KfK 2862.
EUR 6402e (1979).

DE BOLLE, W.E., MÜSCHENBORN, G.,
Small systematic errors from chemical origin in UF_6 isotope measurements during the conversion of UF_6 to UO_3 and the reconversion of UO_3 to UF_6 with COF_3.
GE/NI/MS/40/79.

GEERTS, J., TRIFFAUX, J., VAN AUDENHOVE, J.
Conditioning of non-ferrous reference materials,
Oxygen in Mo (BCR-23) - Oxygen in Ti (BCR-24) - Oxygen in TiAl6V4 (BCR-53).
EUR 6607 (1979).

PAUWELS, J.
The certification of oxygen in non-ferrous metals :
Oxygen in primary ingot aluminium.
EUR 6240 (1979).

PAUWELS, J.
The certification of oxygen in non-ferrous metals :
Oxygen in continuous cast copper rod.
EUR 6421 (1979).

PAUWELS, J.
The certification of oxygen in non-ferrous metals :
Oxygen in titanium-aluminium-vanadium alloy TiAl6V4.
EUR 6242 (1979).

PAUWELS, J.
Intercomparison of analysis methods for oxygen in lead and its alloys.
EUR 6303 (1979).

PAUWELS, J.
The analysis of oxygen and nitrogen in nickel.
EUR 6304 (1979).

QUAGLIA, L., WEBER, G., DAVID, D., TRIFFAUX, J., GEERTS, J., VAN AUDENHOVE, J., PAUWELS, J.
Surface treatment of non-ferrous metals for the purpose of gas analysis.
EUR 6602 (1979).

MISCELLANEOUS

Contribution to conferences

DE KEYSER, A., BABELIOWSKY, T.
A microcontroller based channel simulator for minicomputer connection to an IBM 370 system.
SEAS Anniversary Meeting, SEAS in Conjunction with DESY, Hamburg - F.R. Germany, 24-28 September 1979.

Reports

DEBUS, G.H. (Ed.)
Measurements, standards and reference techniques (METRE).
Summary Programme Progress Report, July-December 1978.

DEBUS, G.H. (Ed.)
Measurements, standards and reference techniques (METRE).
Programme Progress Report, July-December 1978.

DEBUS, G.H. (Ed.)
Measurements, standards and reference techniques (METRE).
Programme Progress Report, January-June 1979.

DEBUS, G.H. (Ed.)
Measurements, standards and reference techniques (METRE).
Summary Programme Progress Report, January-June 1979.

MEYER, H. (Ed.)
ESONE Committee.
Revision of ESONE CAMAC documents
ESONE/DOC/01 - March 1979.

MEYER, H. (Ed.)
(ECA)
CAMAC bibliography.
ECA/GEN/01 - June 1979.

MEYER, H. (Ed.)
(EDISG - ECA)
A technique for the assessment of communication systems for process control.
EDISG/COM.1 - September 1979.

MEYER, H. (Ed.)
(ECA)
CAMAC product Guide - September 1979.

WATTECAMPS, E., BERTHELOT, Ch.
Progress report 1978 - CBNM.
NEANDC(E) - 202(U), Vol. III.
INDC(EUR) -072 G.

ANNEX 2 : CINDA ENTRIES LIST

ELEMENT S	A	QUANTITY	TYPE	ENERGY MIN	MAX	DOCUMENTATION REF	VOL	PAGE	DATE	LAB	COMMENTS
NA	023	N,ALPHA	EXPT-PROG	TR	10+7	INDC(EUR)13	23		680	GEL	WEIGMANN+WNR FACIL AT LASL
NA	023	N,PROTON	EXPT-PROG	TR	10+7	INDC(EUR)13	23		680	GEL	WEIGMANN+WNR FACIL AT LASL
S		TOTAL	EXPT-PROG	10+5	15+7	INDC(EUR)13	20		680	GEL	JUNGMANN+LINAC TOF TRANSM
K	040	N,ALPHA	EXPT-PROG	20-2	70+4	INDC(EUR)13	23		680	GEL	WAGEMANS+LINAC TOF MEAS
K	040	N,PROTON	EXPT-PROG	20-2	70+4	INDC(EUR)13	23		680	GEL	WAGEMANS+LINAC TOF MEAS
FE		N,ALPHA	EXPT-PROG	50+6	10+7	INDC(EUR)13	15		680	GEL	PAULSEN+ANGDIST+E'DIST+SIG
FE	054	TOTAL	EXPT-PROG	35+4	20+6	INDC(EUR)13	11		680	GEL	CORNELIS+
FE	054	N,ALPHA	EXPT-PROG	60+6	17+7	INDC(EUR)13	13		680	GEL	PAULSEN+ACTIV MEAS
FE	054	N,PROTON	EXPT-PROG	60+6	10+7	INDC(EUR)13	13		680	GEL	PAULSEN+ACTIV MEAS
FE	056	TOTAL	EXPT-PROG	35+4	20+6	INDC(EUR)13	11		680	GEL	CORNELIS+
FE	056	N,GAMMA	EXPT-PROG	10+3	10+5	INDC(EUR)13	11		680	GEL	BRUSEGAN+C6D6 DETECTOR
FE	057	TOTAL	EXPT-PROG	35+4	20+6	INDC(EUR)13	11		680	GEL	CORNELIS+
NI		N,ALPHA	EXPT-PROG	50+6	10+7	INDC(EUR)13	15		680	GEL	PAULSEN+ANGDIST+E'DIST+SIG
PD	104	RESON PARAMS	EXPT-PROG	NDG		INDC(EUR)13	20		680	GEL	STAVELOZ+
PD	105	RESON PARAMS	EXPT-PROG	00+0	60+2	INDC(EUR)13	20		680	GEL	STAVELOZ+WN AND WG
PD	106	RESON PARAMS	EXPT-PROG	NDG		INDC(EUR)13	20		680	GEL	STAVELOZ+
PD	108	RESON PARAMS	EXPT-PROG	NDG		INDC(EUR)13	20		680	GEL	STAVELOZ+
PD	110	RESON PARAMS	EXPT-PROG	NDG		INDC(EUR)13	20		680	GEL	STAVELOZ+
U	235	N,GAMMA	EXPT-PROG	+3		INDC(EUR)13	10		680	GEL	CALABRETTA+C6F6 DETECTORS
U	235	N,FISSION	EXPT-PROG	25-2	30+4	INDC(EUR)13	10		680	GEL	WAGEMANS+
U	235	ALPHA	EXPT-PROG	+3		INDC(EUR)13	10		680	GEL	CALABRETTA+C6F6 DETECTORS+FISS CHB
U	238	RESON PARAMS	EXPT-PROG	50+3	10+5	INDC(EUR)13	9		680	GEL	MOORE+S AND P WAVE IDENTIF
PU	239	N,FISSION	EXPT-PROG	25-2	30+4	INDC(EUR)13	7		680	GEL	WAGEMANS+
PU	239	FRAG SPECTRA	EXPT-PROG	20-2	10+6	INDC(EUR)13	7		680	GEL	WAGEMANS+FRAG ENERGY+MASS DISTR
PU	240	N,FISSION	EXPT-PROG	10+4	30+5	INDC(EUR)13	6		680	GEL	BUDTZ-JORGENSEN+TOF MEAS LINAC
PU	240	N,FISSION	EXPT-PROG	14+5	98+6	INDC(EUR)13	5		680	GEL	BUDTZ-JORGENSEN+TOF MEAS VDG
AM	241	ABSORPTION	EXPT-PROG	50+0	10+2	INDC(EUR)13	5		680	GEL	VAN PRAET+
AM	241	N,FISSION	EXPT-PROG	50+0	10+2	INDC(EUR)13	5		680	GEL	VAN PRAET +

ANNEX 3 : LIST OF RESIDENT AND VISITING SCIENTIFIC AND TECHNICAL STAFF

JRC-Geel Staff

Director : Batchelor R.

Division Heads :

Research : Rose B.
Administration and Infrastructure : Gubernator K.

Group Leaders : Bambynek W.
Böckhoff K.H.
De Bièvre P.J.
Eschbach H.L.
Horstmann H.
Liskien H.
Meyer H.
Van Audenhove J.
Leurs U.

Scientific Secretariat :
Debus G.H.

Health Physics :
de Ras E.

Aerts M.
Arnotte F.
Babeliowsky T.
Barthelemy R.
Bastian C.
Bax H.
Beckers F.
Berthelot Ch.
Besenthal R.
Blockx E.
Borgers R.
Bortels G.
Bouwens J.
Bouwmeester E.
Broothaerts J.
Brusegan A.
Budtz-Jørgensen C.
Buyl R.
Carraro G.
Celen E.
Cervini C.
Ceunen L.
Claes K.
Cools H.
Cools R.
Corvi F.
Crametz A.
Daems F.
Daems L.
Daems P.
Damen
Danckers G.
De Backer L.
De Bolle W.
De Buck A.
de Jonge S.
De Keyser A.
De Pooter D.
De Roost E.
De Spiegeleer A.
Deckx J.
Denecke B.
Dijckmans B.
Dijckmans M.
Dobma W.D.
Dufrasnes A.
Ehrenfreund G.
Falque P.
Forni R.
Freisted E.
Gallet M.
Geeraerts R.
Geerts K.
Gelly D.
Grosse G.
Hansen H.
Hendrickx F.
Hens E.
Herrmann S.
Hofmans K.
Idzerda B.
Jacobs G.
Janssens V.
Kacperek A.
Kennis W.
Klopf P.
Knitter H.H.
Le Dez G.
Le Duigou Y.
Leidert W.
Leonard J.
Loopmans A.
Louwerix E.
Luyten F.
Lycke W.
Maes F.
Mailly M.
Massardier F.
Mast H.
Mast J.
Melis F.
Melis G.
Meloni U.
Mencarelli T.
Mensch H.
Menu F.
Merla M.
Meynants K.
Michiels A.
Michiels E.
Mitchell I.V.
Moore M.
Mouchel D.
MÜschenborn G.
Nagel W.
Nerb H.
Nijs R.
Noyens J.
Noyens Jos.
Nylandsted-Larsen A.
Oldenhof W.
Parduyns G.
Parengh M.
Paulsen A.
Pauwels J.
Peetermans F.
Pijpstra R.
Prins H.
Quik F.
Reher D.
Renders I.
Rietveld P.
Rohr G.
Ruts H.
Ryngaert E.
Salomé J.M.
Sattler E.
Schipke H.
Schreiber W.
Segers F.
Sempeis J.
Shelley R.
Silvester H.
Siméone P.
Smets R.
Stal B.
StÜber W.
ter Meer P.
Teuling C.
Tjoonk J.
Traas L.
Triffaux J.P.
Uijlenbroek B.
Van Baelen F.
Van Baelen G.
Vanberghen C.
Van Bijlen J.
Van Bijlen R.
V.Broekhoven A.
V.Broekhoven W.
van de Beek H.
Vandevelde S.
Van de Vonder R.
Van der Veen T.
Van Duffel E.
Van Endert J.
Van Gestel J.
Van Gorp A.
Van Hengel L.
V.Heuckelom W.
Vaninbroukx R.
V.Overstraeten J
Van Reeth F.
Van Rhee L.
Van Rillaer C.
Van Roy P.
Van Saene J.
Vansant J.
V.Suetendael W.
V.Waelderen H.
Verdingh V.
Verdonck J.
Verheyen F.
Verwimp R.
Vogt R.
Waelbers J.
Waller C.
Wartena J.
Wattecamps E.
Weigmann H.
Werz R.
Widera R.
Winter J.
Wolters W.
Zehner W.